MICROCOPY RESOLUTION TEST CHART

NATIONAL BUREAU OF STANDARDS-1963-A

STUDY OF A TUNABLE CO_2/N_2O

MEDIUM PRESSURE WAVEGUIDE LASER

THESIS

AFIT/GEO/PH/83D-1   Adam R. Bigelow
2nd Lt.   USAF

DEPARTMENT OF THE AIR FORCE
AIR UNIVERSITY
AIR FORCE INSTITUTE OF TECHNOLOGY

Wright-Patterson Air Force Base, Ohio

84 02 21 173

STUDY OF A TUNABLE CO_2/N_2O

MEDIUM PRESSURE WAVEGUIDE LASER

THESIS

AFIT/GEO/PH/83D-1   Adam R. Bigelow
                      2nd Lt.   USAF

Approved for public release; distribution unlimited.

DTIC
ELECTE
FEB 2 2 1984

A

AFIT/GEO/PH/83D-1

STUDY OF A TUNABLE CO_2/N_2O
MEDIUM PRESSURE WAVEGUIDE LASER

THESIS

Presented to the Faculty of the School of Engineering

of the Air Force Institute of Technology

Air University

in Partial Fulfillment of the

Requirements for the Degree of

Master of Science

by

Adam R. Bigelow, B.S.

2nd Lt.   USAF

Graduate Electro-Optics

December 1983

Acknowledgements

I would like to acknowledge the guidance and assistance of Mr. Charles A. DeJoseph who proposed this thesis and patiently endured my many questions. He taught me many of the techniques needed for this experiment, and saved me innumerous frustrations by pointing me in the correct directions. My appreciation also goes to my faculty advisor, Lt. Col. William Bailey, who offered me advice and gave me a free reign in the laboratory as I conducted the experiment. Finally, I would like to thank my fiancé, Paula Johnson, for her loving support and understanding and for the personal sacrifices she made while I was completing this project.

Adam R. Bigelow

Table of Contents

List of Figures

Abstract

The operational characteristics of a CO_2 waveguide laser, capable of both inter-line and intra-line tuning, were investigated. This system based on the design of Gerlach and Amer (Ref 14) exhibits an overall simplicity in design and construction. In addition, only inexpensive and readily available materials are required. The range of gas pressures in the discharge extended from 25 Torr to 162 Torr while using a 20/10/70 gas mixture of CO_2/N_2/He. The P(20) line, which was scanned using a piezoelectric transducer, had a tunable linewidth of 215 MHz. This linewidth was limited by the 220 MHz free spectral range of the cavity. In the multi-line configuration, the maximum output was 7.5 W. A grating was used to achieve inter-line tuning; a total of 50 different lines of the P and R branches of the 10.4 m and 9.4 m lased. A maximum output power of 2.2 W, P(20), was achieved during single line operation. A 9.9/9.8/80.3 gas mixture of N_2O/N_2/He was also investigated. In the multi-line configuration a maximum output of 825 mW was achieved.

vi

I   INTRODUCTION

Background

A low power (a few watts) Carbon dioxide/Nitrous oxide (CO_2/N_2O) waveguide laser would be useful both for optoacoustic and optogalvanic studies of some gases used in semiconductor plasma deposition. Both inter-line and intra-line tuning are needed for these experiments. A novel CO_2/N_2O waveguide laser has been constructed by Gerlach and Amer (Ref 14) using relatively inexpensive materials and simple construction.

Problem Statement

The goal of the study was to build a CO_2/N_2O wave-guide laser following the basic design of Gerlach and Amer. The laser was to be capable of both inter-line and intra-line tuning.

Scope and Approach

This study was concerned initially with reproducing the work of Gerlach and Amer. They presented a new design for a waveguide laser which was extremely simple and could be built from relatively inexpensive materials that were readily available. The laser operates in a multi-line configuration (using either CO_2 or N_2O) or can be used for inter-line tuning (with CO_2). Therefore, the first

part of this project was to determine if this type of laser (once constructed) would prove to be a useful tool in the laboratory.

Secondly, this thesis extended the work of Gerlach and Amer. A piezoelectric transducer (PZT) was used to change the length of the resonator in order to determine the feasibility of intra-line tuning with the new and simple laser design. Investigation of intra-line tunability was conducted only on the P(20) line of CO_2. Since Gerlach and Amer were unable to achieve inter-line tuning using N_2O as the lasing medium, part of the study also included the attempt to lase with N_2O in the single line configuration.

The experimental study can be broken into four major areas:

1)   Design and construction of the laser

2)   Optimizing the laser

3)   Inter-line tuning

4)   Intra-line tuning

1) Design and construction of the laser. The design of the laser closely followed the design of Gerlach and Amer. The materials chosen for the laser accomplished a 3-fold purpose. First, the materials were chosen to reproduce the design of Gerlach and Amer as closely as possible. Secondly, the materials were inexpensive and readily

available. Finally, any of the components that were
manufactured, were simple and easy to make. Once the
individual components of the laser were gathered and/or
constructed, they were mounted onto a small U-channel.
The U-channel, with the laser mounted on it, coul᷎ be
easily transported and bolted to any standard oϼ cal air
table. A detailed description of the constructi and
assembly of the waveguide laser is found in Chap ᷎ III of
this thesis.

2) Optimizing the laser. The laser was optimized for
maximum output power while in the multi-line configura-
tion. The pressure of the gas in the discharge tube was
varied to find the maximum laser output. The discharge
current and mirror spacing were also varied. Lastly, the
output coupler was adjusted until the optimum was
identified. The multi-line lasing configuration (i.e. no
grating) experiment and results are discussed in the first
section of Chapter IV.

3) Inter-line tuning. A grating replaced the total
reflector of the multi-line cavity in order to investigate
the inter-line tuning characteristics of the laser. When
the grating was rotated and the laser beam fed into a
spectrometer, various lasing lines were observed and
recorded. The results of inter-line tuning can be found
in the second major section of Chapter IV.

4) Intra-line tuning. The output mirror of the laser was mounted in a PZT. The P(20) line of CO_2 was scanned as a ramp voltage was applied to the PZT. The width of the line was measured using a fast detector and a low pressure gas absorption cell. Results of intra-line tuning are presented in the third section of Chapter IV of this thesis.

Waveguide laser design theory is discussed in Chapter II. Also included in the chapter are overviews of the CO_2 and N_2O lasing processes as well as brief descriptions of the inter-line and intra-line tuning processes. Finally, in Chapter V, conclusions are presented on the waveguide laser and recommendations for improvements in each of the three configurations (multi-line, inter-line, and intra-line) are made.

II THEORY

The purpose of this thesis is experimental in nature.
The theory portion of this thesis provides the reader with
a basic understanding of how a CO_2 waveguide laser works.
While the theory presented is general in nature, some
emphasis is placed on those elements which were used in the
present thesis (i.e., external reflectors were used to form
a resonator, therefore, discussion on resonator designs are
limited to resonators with external reflectors).

The chapter begins with a discussion of a conventional
resonator and then moves to a description of the modes a
waveguide will support, and waveguide resonator design
theory. An overview of the CO_2 and N_2O lasing pro-
cesses is also given along with a presentation of inter-
line and intra-line tuning theory. The chapter concludes
with some remarks on the losses expected in an operating
laser system.

The Conventional Gas Resonator

The CO_2 waveguide laser shares some of the same
characteristics as a conventional electric discharge CO_2
gas laser; both have a discharge tube, a power supply, and
some sort of laser cavity. In a standard gas laser (see
Fig. 1), the discharge tube is placed between two mirrors
forming a Fabry-Perot cavity. One mirror is a total

reflector, while the other mirror is partially transmissive
in order to extract some of the lasing energy. The total
reflector does not have to be a mirror; it could be another
optical element, such as a reflective grating. The length
of a stable Fabry-Perot laser cavity is determined by the
radii of curvature of the two mirrors.

Siegman (Ref 1:300) states that an optical resonator
is stable if

$$0 \leq g_1 g_2 \leq 1 \qquad (1)$$

where $g_1 g_2$ are called the g parameters and

$$g_i \equiv 1 - \frac{L}{R_i} \qquad (2)$$

L is the total cavity length and R_i is the radius of
curvature of the ith mirror (i = 1 or 2). Using Eqs (1)
and (2) it can be shown that for a stable cavity the maxi-
mum length L can be is

$$L = R_1 + R_2 \qquad (3)$$

The discharge tube, for a longitudinally flowing gas
laser, consists of a cylindrical tube (often Pyrex), gas
ports, Brewster windows, and electrodes. The gas ports

-6-
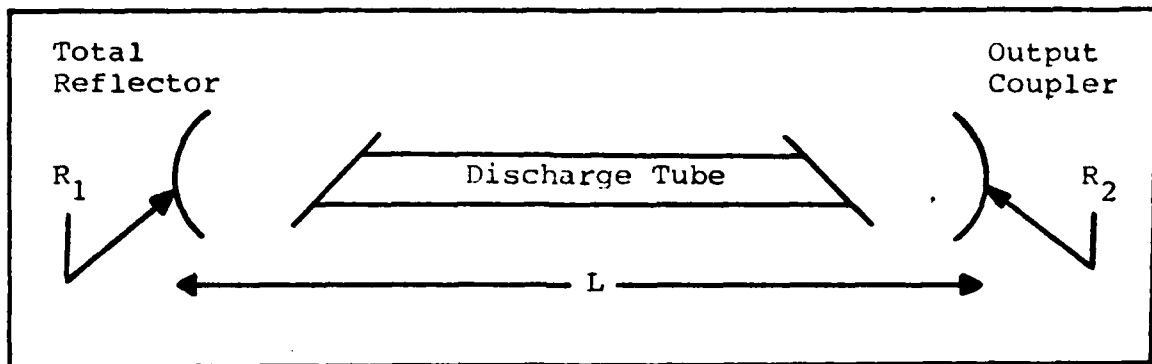
Figure 1.   Standard Gas Laser

are necessary to flow the gas in and out of the tube.   Some
gas lasers can be run sealed off, while some uses dictate
the need to exhaust the used gas.   The Brewster windows
mounted on the end of the discharge tube are used to
linearly polarize the emitted light.   Finally electrodes
are necessary in order to create a D.C. discharge, which
in turn, excites the gas and produces lasing action.

The Waveguide Laser

A waveguide laser can be distinguished from a conven-
tional laser by the characteristic that, over some portion
of the propagation path, the radiation within the laser
cavity is guided by means of a waveguide and does not obey
the laws of free space propagation.   As a consequence,
conventional resonator theories, which are derived under
the assumption of free space propagation between two re-
flecting surfaces, do not adequately describe the frequency
spectra, losses, spatial mode distributions, or stability
conditions characteristic of waveguide lasers.   Common

materials for the waveguide are Beryllium Oxide (BeO) and Alumina (Al_2O_3). BeO gives off a toxic dust when machined and hence requires special safety precautions during fabrication. Al_2O_3 is inferior to BeO in its thermal and waveguide properties, but it does not require special handling during fabrication (Ref 2:24).

In many waveguide lasers, the discharge tube serves as the waveguide. Figure 2 shows a Fabry-Perot cavity with a waveguide and external mirrors. Various geometries for the waveguide cross-section exist, but the present thesis will focus on circular cross-sections only. The following discussion (adapted from Ref 2) describes the nature of the waveguide and the modes expected in a hollow cylindrical guide.

The modes of hollow cylindrical dielectric waveguides having diameters much larger than a wavelength were first derived by Marcatili and Schmeltzer (Ref 3). The allowed modes fall into three categories: transverse circular electric (TE_{0m}), transverse circular magnetic (TM_{0m}), and the hybrid modes EH_{nm} where the integer n may take on negative as well as positive values and $|n| \geq 1$. In addition to the assumption of guide diameters large compared to wavelength, the theory is also restricted to low-order, low-loss modes whose propagation constants are nearly equal to the plane wave value. Fairly complex
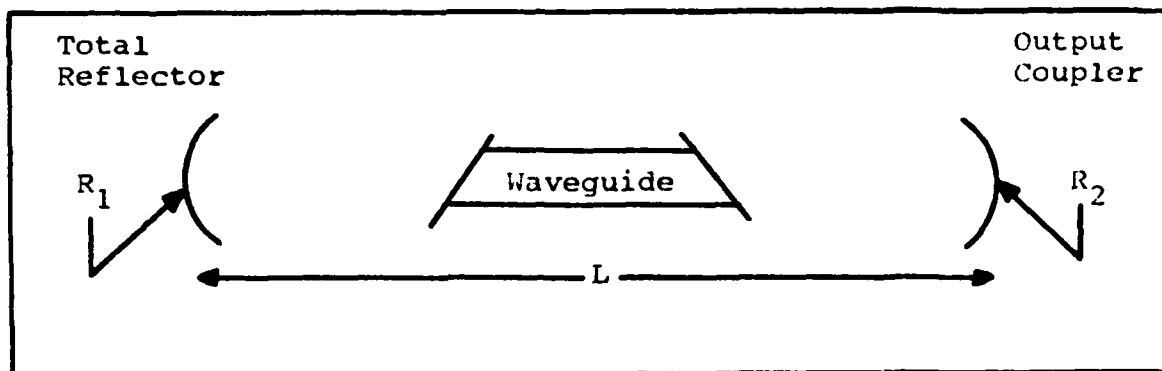
Figure 2. Fabry Perot Waveguide Laser

approximations for the field components containing terms up to and including order λ/a have been derived by Degnan and others (Refs 3,4) where λ is the wavelength and a is the radius of the guide. To this order of approximation, the z components of electric and magnetic field for the hybrid EH_{nm} modes do not vanish. However, if one considers guides sufficiently large so that terms of order λ/a may be ignored, the fields approach the simple TEM-like solutions given below.

Circular Electric Modes $TE_{0m} (m \geq 1)$

$$E_\phi = J_1 \left(\frac{U_{0m}r}{a} \right) e^{i(\gamma z - wt)}$$

$$H_r = - \sqrt{\frac{\varepsilon_0}{\varepsilon_0}} \ E_\phi \tag{4}$$

$$H_z = 0(\lambda/a)$$

Circular Magnetic Modes $TM_{0m} (m \geq 1)$

$$E_r = J_1\left(\frac{U_{0m}r}{a}\right) e^{i(\gamma z - wt)}$$

$$H_\phi = \sqrt{\frac{\epsilon_0}{\mu_0}} \; E_r \qquad\qquad (5)$$

$$E_z = 0(\lambda/a)$$

Hybrid Modes $EH_{nm} (n \neq 0, \; m \geq 1$

$$E_\phi = J_{n-1}\left(\frac{U_{nm}r}{a}\right) \cos(n\phi)$$

$$\left. \vphantom{\begin{array}{c}1\\1\\1\end{array}} \right\} e^{i(\gamma z - wt)}$$

$$E_r = J_{n-1}\left(\frac{U_{nm}r}{a}\right) \sin(n\phi) \qquad\qquad (6)$$

$$H_\phi = \sqrt{\frac{\epsilon_0}{\mu_0}} \; E_r$$

$$H_r = \sqrt{\frac{\epsilon_0}{\mu_0}} \; E_\phi$$

$$E_z = 0(\lambda/a)$$

$$H_z = 0(\lambda/a)$$

where U_{nm} is the mth root of the equation

$$J_{n-1} = (U_{nm}) = 0 \qquad (7)$$

and the notation $0(\lambda/a)$ implies that the particular field component is reduced in magnitude relative to the principal components by an approximate factor of λ/a. The lowest order approximation to the field components given in Eqs (4) through (6) are of interest since they form the basis for existing theories of waveguide laser resonators to be discussed later. Unlike the latter equations, the higher-order approximations describe fields which do not quite vanish at the guide boundary (Ref 3,4) but decay exponentially within a thin segment of the waveguide wall (Ref 3). The electric field lines and amplitude distributions for the various modes are plotted in Figure 3 (adapted from Degnan) where it may be noted that the EH_{im} modes are linearly polarized and have circularly symmetric amplitude functions. The propagation constant λ in Eqs (4) through (6) are given by (Ref 3)

$$\gamma = k \left[1 - \frac{1}{2} \left(\frac{U_{nm}}{ka} \right)^2 \left(1 - \frac{i2\nu n}{ka} \right) \right] \qquad (8)$$

-11-
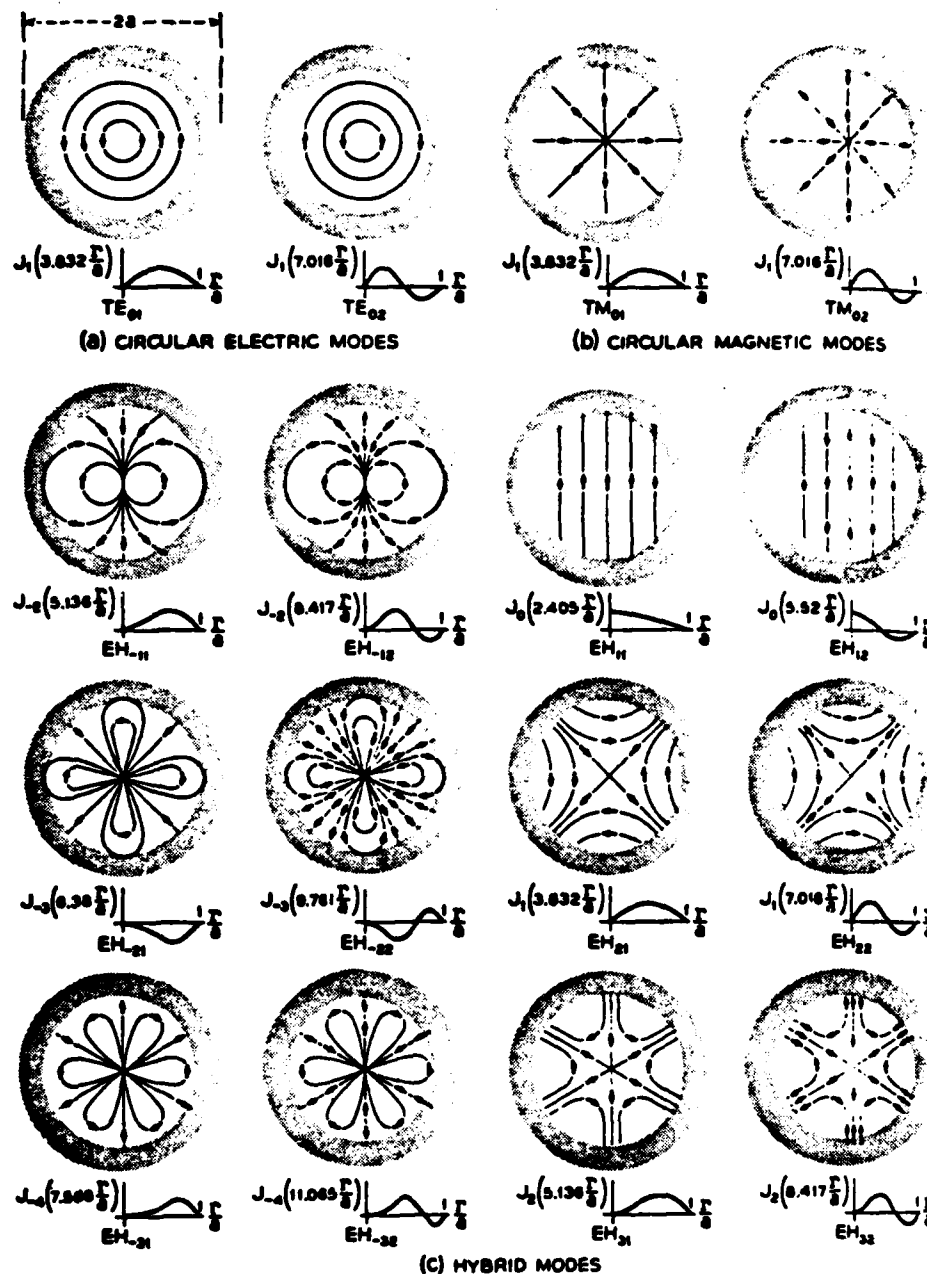
Figure 3. Electric field modes in hollow dielectric
waveguide (Ref 2)

where $k = 2\pi/\lambda$ is the propagation constant for an infinite plane wave in the core material,

$$\nu_n = \begin{cases} \dfrac{1}{\nu^2-1} & \text{for TE}_{0m} \text{ modes } (n = 0) \\[3mm] \dfrac{\nu^2}{\nu^2-1} & \text{for TM}_{0m} \text{ modes } (n = 0) \\[3mm] \dfrac{\nu^2+1}{2\nu^2-1} & \text{for EH}_{nm} \text{ modes } (n \neq 0) \end{cases} \qquad (9)$$

and where $\nu = \varepsilon_1 / \varepsilon_0$ where ε_1 and ε_0 are the complex susceptabilities of the external and internal media respectively. The real part of the propagation constant γ is therefore

$$\beta_{nm} = \text{Re}\{\gamma\} = \frac{2\pi}{\lambda_{nm}}$$

$$= k \left[1 - \frac{1}{2}\left(\frac{U_{nm}}{k\alpha}\right)^2 \left(1 + \frac{2}{k\alpha}\right) \text{Im}\{\nu_n\} \right] \qquad (10)$$

Where λ_{nm} is the guide wavelength of radiation in the mode described by the integers n and m. The attenuation of the modes in the guide is given by the imaginary component, that is

$$\alpha_{nm} = \text{Im}\{\gamma\} = \left(\frac{U_{nm}}{k}\right)^2 \frac{1}{\alpha^3} \text{Re}\{\nu_n\} \qquad (11)$$

-13-

The mode with lowest attenuation is TE_{01} if $\nu > 2.02$ and EH_{11} if $\nu < 2.02$. The increased attenuation due to curved guides has been considered by Marcatilli and Schmeltzer (Ref 3). Additional losses can be caused by surface roughness.

Waveguide Resonator Design (External Mirrors)

A waveguide laser utilizing external mirrors may be modeled by considering each end of the waveguide as a radiating source whose electric field distribution is a valid solution of Maxwell's equations satisfying the wave-guide boundary conditions, i.e., a linear combination of allowed waveguide modes discussed above. Each mirror then acts as a feedback element, coupling a portion of the radiation back into one or more waveguide modes and scattering the remainder beyond the guide aperture.

The far field pattern of the EH_{11} mode, shown in Figure 4, contains over 98% of its energy in a central lobe, is circularly symmetric, and is linearly polarized. The normalized intensity is plotted against the parameter $k_0 ax/d$ where k_0 is the free space propagation constant, a is the guide radius, x is one of the transverse cartesian coordinates in the observation plane, and d is the distance from the guide exit to that plane. Unlike the gaussian mode of conventional resonators, the far-field pattern of

-14-

(4)

(5)
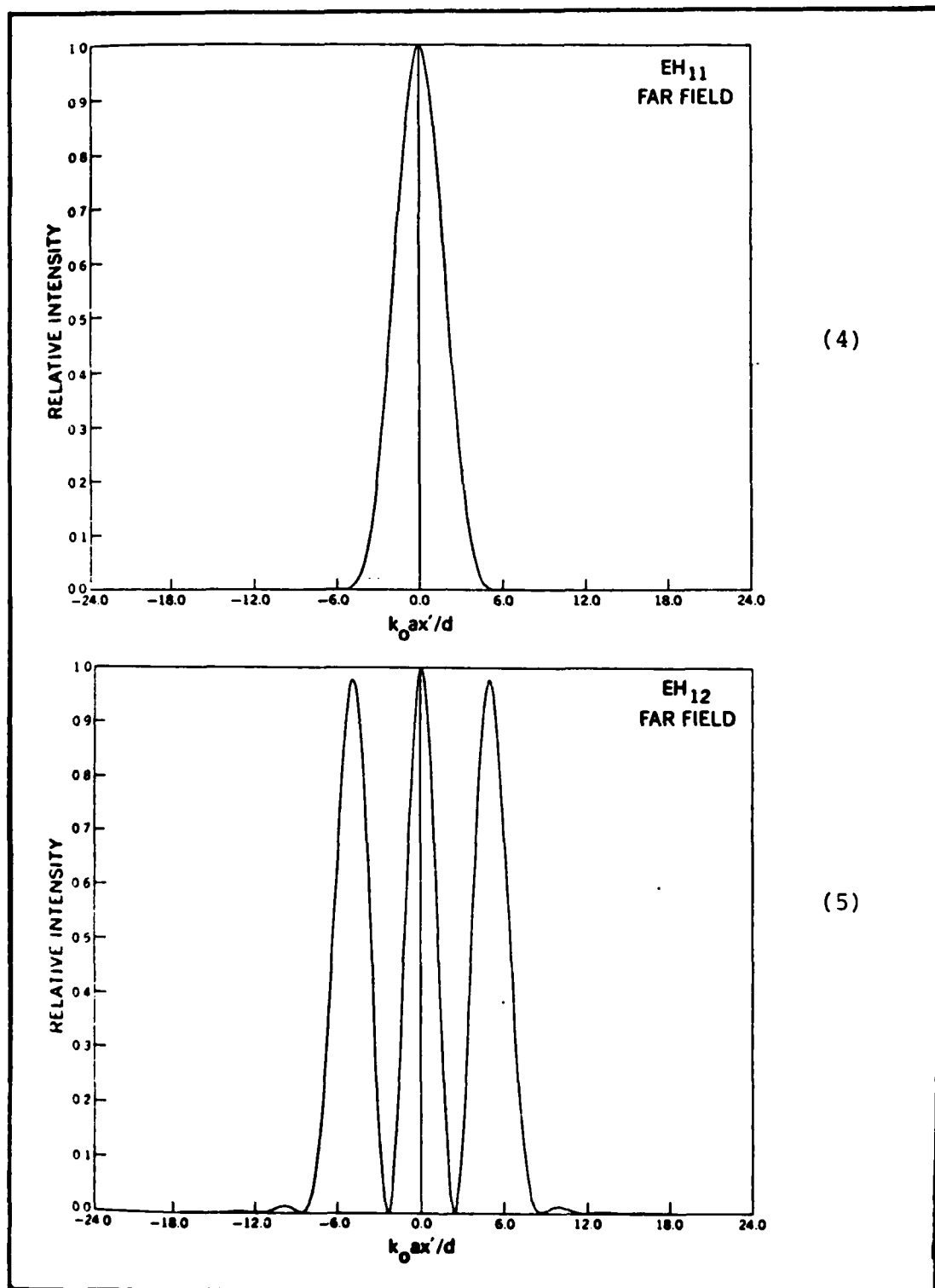
Figures 4 and 5. Far Field Patters (Ref 2)

the fundamental waveguide mode EH_{11} has several weak
concentric rings surrounding the central lobe which result
from the assumption that the electric field is identically
zero at the guide boundry (Ref 2:10). Figure 5 shows the
EH_{12} mode which has most of its energy contained in
three main lobes.

Since a resonator mode dominated by the EH_{11} wave-
guide mode is desirable for most applications (most of
energy in a single lobe), it is of interest to determine
those mirror configurations which efficiently couple the
EH_{11} mode back into the guide (Ref 2:10). Several
authors, Abrams (Ref 5) and Degnan and Hall (Ref 6) have
computed the fraction of energy returned to the guide in
the EH_{11} mode after the same mode has been launched into
free space and returned to the guide by an external
spherical reflector. The EH_{11} coupling loss is plotted
(see Fig. 6) as a function of a normalized mirror separa-
tion z/b and a normalized mirror curvature R/b where b is
the confocal parameter of the gaussian beam which best
approximates the field distribution of the EH_{11} wave-
guide mode. The confocal parameter of the "approximating
gaussian" is defined by

$$b = \pi \, \omega_0^2 / \lambda_0 \qquad (12)$$
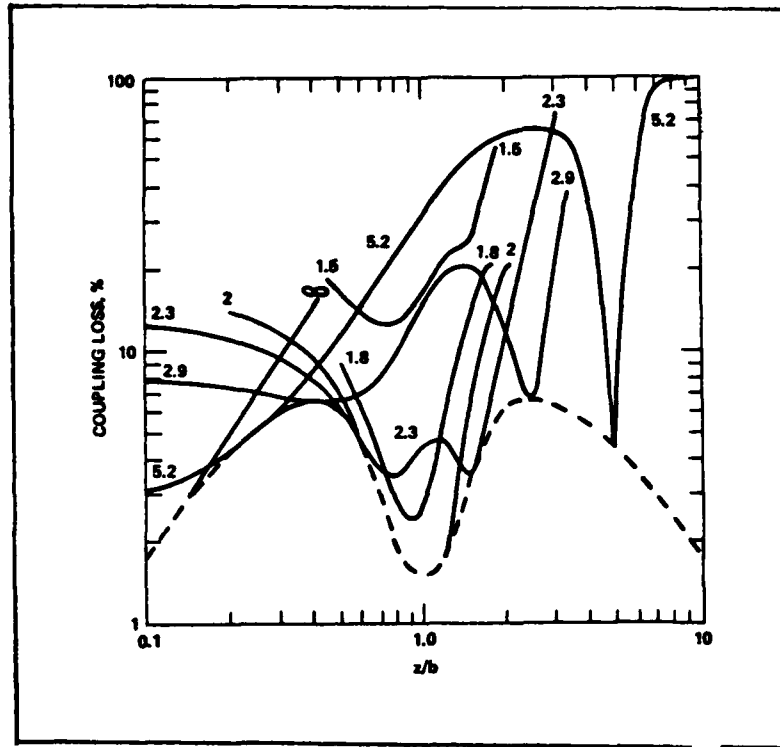
Figure 6. EH_{11} coupling loss (Ref 2)

where λ_0 is the free-space wavelength and

$$\omega = 0.6435 \, \mathcal{Q} \qquad (13)$$

is the radius of the gaussian beam waist which maximizes

the overlap integral of a gaussian with the EH_{11} mode

distribution in a circular guide of radius $\mathcal{Q}$. The phase

front curvature at a distance z from the gaussian beam

waist is given by conventional resonator theory (Ref 7) as

$$R' = b \left(\frac{z}{b} + \frac{b}{z} \right) \qquad (14)$$

Efficient coupling would be expected when the mirror curvature matches the wavefront curvature since all rays would be directed back onto themselves. The dashed curve in Figure 6 gives the EH_{11} coupling loss under the assumption that the mirror curvature matches the phase-front curvature of the approximating gaussian beam at each mirror separation z. It may be noted that the individual solid curves in the figure, each of which corresponds to a particular mirror curvature, touch the dashed curve at two points for "large" curvatures (R/b > 2) and not at all for smaller curvatures (R/b < 2). This occurs because Eq (14) has a minimum value of $R_{min} = 2b$ at a distance z = b from the guide. Thus for a mirror curvature R > R_{min} (R/b > 2) there are two mirror positions on opposite sides of z = b (z/b = 1) where the mirror curvature matches the phasefront. For R < R_{min} (R/b < 2), however, no match is possible and, as expected, the losses for these smaller curvatures are relatively high. The latter losses are minimized, however, at mirror separations which are half the radius of curvature from the guide.

Degnan and Hall (Ref 6:904) have calculated the EH_{11} coupling efficiency as a function of the parameters

$$\alpha = k_0 a^2/R \qquad \beta = z/R \qquad \gamma = D/2a \qquad (15)$$

-18-

where $k_0 = 2\pi/\lambda_0$ and D is the mirror diameter (assumed equal to ∞ in the Abrams calculations). In general, there are three low loss ($< 2\%$) configurations for the EH_{11} mode:

I) Flat mirrors close to the end of the guide entrance ($R/b = \infty$, $z/b = 0.1$ or $\alpha = 0$, $\beta \approx 0$).

II) Large radius of curvature mirrors whose centers of curvature lie approximately at the guide entrance ($z \approx R \gtrsim 8b$ or $\alpha \lesssim 0.6$, $\beta \approx 1$).

III) Shorter radius of curvature mirrors at a distance one-half the radius of curvature from the guide ($R/b = 2$, $z/b = 1$ or $\alpha = 2.416$, $\beta = 0.5$).

In Case I, 100% coupling efficiency is achieved for all waveguide modes by placing the flat directly against the guide. Moving the flat a small distance z from the guide entrance introduces an EH_{11} coupling loss given by

$$L = 57\left(\frac{z}{b}\right)^{3/2}[\%], \text{ for } z/b \lesssim 0.4 \qquad (16)$$

Case II is also relatively easy to understand. At a sufficiently large distance from the waveguide aperture, the launched waveguide mode evolves into its far-field distribution with spherical wavefronts centered approximately at the guide entrance. If a spherical mirror having a curvature matching the phasefront is placed at

-19-

that position, the electric field is imaged back onto itself with near perfect fidelity. Transverse mode discrimination can be provided by limiting the aperture of the external mirror. Computation of the EH_{11} and EH_{12} coupling loss as a function of mirror curvature and aperture as well as curves showing the sensitivity of the coupling efficiency to mirror separation for this configuration have been presented by Degnan and Hall (Ref 6).

In Case III, the mirror is sufficiently near-field relative to the guide so that the curvature of the impinging wavefront differs significantly with waveguide mode number. Thus, unlike the EH_{11} mode, higher order waveguide modes are not coupled with high efficiency back into the guide. (Higher order modes diverge more rapidly than the fundamental EH_{11} mode.) Specifically it has been shown (Ref 6:906) that, while the EH_{11} mode suffers a coupling loss of only 1.4%, the EH_{12} mode loss is about 78%. Thus Case III is interesting because it provides excellent transverse mode discrimination even with large mirror apertures.

Returning to the curves of Figure 6, we note that, on the basis of EH_{11} losses alone, one would expect, at most, two laser output power maxima as a particular mirror is moved relative to the guide. In actual experiments, many maxima are observed, and it has been shown (Refs 6,8)

-20-

that the additional power maxima occur at separations which strongly couple the EH_{11} mode to higher order EH_{1m} waveguide modes. In particular, power maxima have been experimentally observed in configurations in which the mirror separation is approximately equal to or greater than the curvature of the mirror (adapted from Ref 2).

CO_2 Lasing Process

The following section will provide the reader with an overview of the CO_2 lasing process. Topics in the overview include: molecular structure, energy level diagrams, pumping mechanisms, laser transitions, and the de-excitation of the lower lasing levels.

The carbon dioxide molecule is a linear triatomic molecule. There are three normal modes of vibration: symmetric stretching (v_1), bending (v_2), and asymmetric stretching (v_3) (see Fig. 7). The oscillation behavior is therefore described by the quantum numbers n_1, n_2, and n_3, which give the number of quanta in each vibrational mode. The corresponding level is designated by the three quantum numbers written in the order n_1, n_2, n_3. For example, the 010 level corresponds to an oscillation in which there is one vibrational quantum in mode 2. Laser action generally occurs between the 001 and 100 levels (10.4 m band) as well as between

-21-
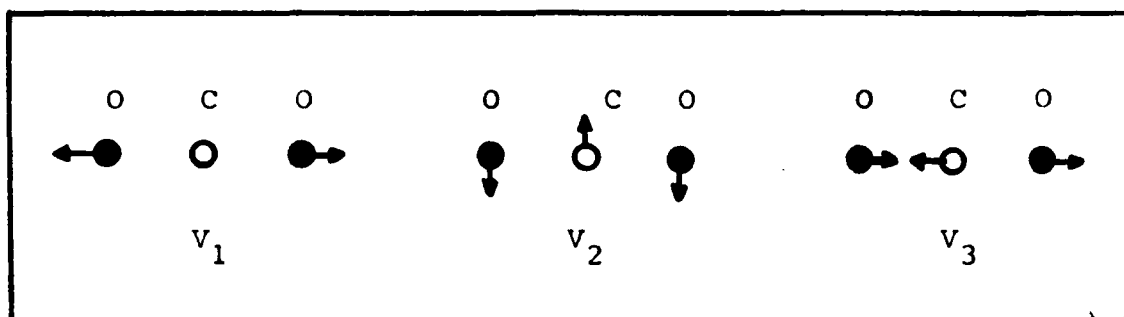
Figure 7. Normal modes of vibration for a CO_2 molecule

the 001 and 020 levels (9.4 um band) (Ref 9). These
energy levels are illustrated in Figure 8.

Lasing occurs between vibrational-rotational levels in
the ground electronic stage of CO_2. The rotational
levels are omitted from Figure 8 for simplification.
However, this detailed energy level structure is high-
lighted in Figure 9. For each vibrational level (i.e.,
the 001, or 010), there exists a band of rotational levels.
A particular rotational level is designated by a rotational
quantum number J. The population of the rotational levels
is described by Boltzman distribution, and in the ground
electronic state, the odd rotational levels are absent
(Ref 10:120). Laser transistions from rotational level
(J) to (J + 1) are called P branch transitions, while
transitions from (J) to (J - 1) are called R branch (see
Fig. 9).

The excitation of CO_2 usually occurs in an electric
discharge which, in addition to CO_2, typically contains
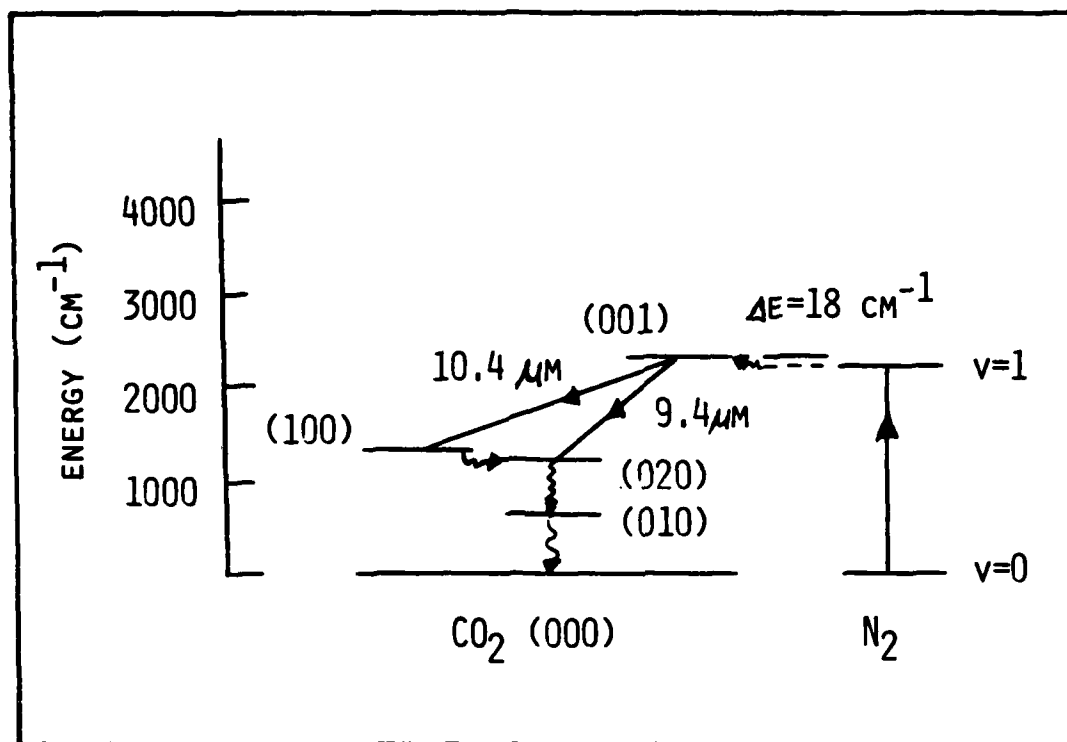
Figure 8. Lowest vibrational levels of a ground electronic
state

N_2 and He. The CO_2 laser possess a high overall

efficiency of about 30 percent. This efficiency results

primarily from three factors.

i) The laser levels are all near the ground state,

and the quantum efficiency is about 45 percent.

ii) A large fraction of the CO_2 molecules excited

by electron impact cascade down the energy ladder from

their original level of excitation and tend to collect in

the long-lived 001 level (Ref 18:174). This occurs through

collisions with ground state CO_2 molecules in the

following (nearly) resonant process (Ref 9:221):
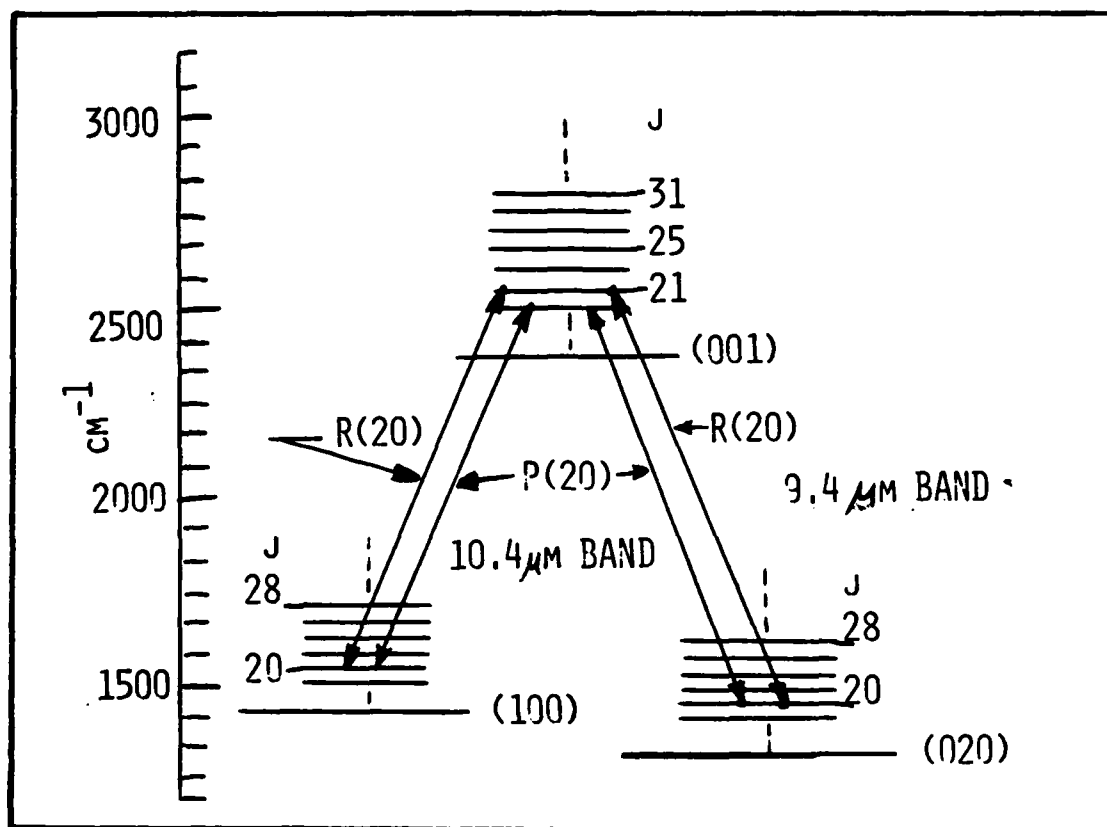
Figure 9. Detailed Laser Transition for the 001-100 and
001-020 bands, including rotational levels

$$(0,0,n) + (0,0,0) \rightarrow (0,0,n-1) + (0,0,1) \qquad (17)$$
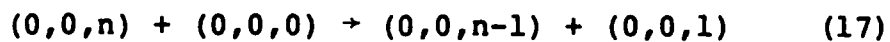
iii) A very large fraction of the N_2 molecules that
are excited by the discharge tend to collect in the $v = 1$
level. Collisions with ground state CO_2 molecules result
in transferring their excitation to the latter, thereby
exciting the CO_2 to the 001 state as shown in Figure 8.
The slight difference in energy, about 18 cm^{-1}, is made
up by a decrease of the total kinetic energy of the mole-
cules following the collision (Ref 18:174).

-24-

We have seen that N_2 is used to excite CO_2 molecules to the upper lasing levels. Helium is added to the gas mixture to relax the lower lasing level of CO_2. Returning once again to Figure 8, it can be seen that the relaxation process involves a number of levels. The 010 level is the most critical since the relaxation of this level limits the laser transitions and creates a bottle-neck. However, the admittance of He into the gas mixture drastically reduces the relaxation time of the 010 level, and the bottleneck is removed (Ref 9:222).

In the CW mode of operation, there are two major lasing transitions: the 10.4 μm band and the 9.4 μm band. Laser transitions between the 001 and 100 levels make up the 10.4 μm band. P branch transitions vary from 10.4 μm to 11.1 μm, while R branch transitions vary from 10.0 μm to 10.4 μm. Laser transitions between the 001 and 020 levels make up the 9.4 μm band. P branch lines vary from 9.4 μm to 9.9 μm, while R branch lines vary from 9.1 to 9.4 μm. Other lasing bands exist, but are much weaker than those mentioned above, and most of them oscillate only under pulsed excitation.

Overview of the N_2O Lasing Process

The N_2O (Nitrous Oxide) lasing process, in many ways is very similar to the CO_2 lasing process. Both involve

linear triatomic molecules with vibrational-rotational
lasing transitions in the IR. Both are pumped by resonant
energy transfer of N_2, and both are de-excited by helium
in the lower lasing levels. There are, however, some
differences. The N_2O laser has experimentally proven to
be less efficient (laser power out vs. input power) than
the CO_2 laser (Ref 14:1540). A second difference is that
the N_2O laser has twice as many allowed vibrational-
rotational transitions (i.e. more lasing transitions),
because the odd rotational levels absent in the ground
electronic state of CO_2, are present in N_2O. Lastly,
there is a slight shift of the band centers of the lasing
lines. The band centers for N_2O are at 10.65 μm and
9.47 μm vs. 10.40 μm and 9.40 μm for CO_2 (Ref 11).

Inter-Line Tuning

It has been shown (Ref 10:167) that the rotational
levels of CO_2 compete strongly for lasing. As a result,
oscillation often switches from one line to the next,
especially in a high power laser system without a disper-
sive element. Therefore, if it is desired to lase on a
single line, a dispersive element must be used, i.e., a
prism or a grating. Since a reflection grating can be
used as the total reflector in a resonator (which was often
the case in the present thesis), discussion will be limited
to the grating.

A grating disperses energy according to the grating equation

$$m \lambda = a(\sin\Theta_m - \sin\Theta_i) \qquad (18)$$

where

m	$\equiv$	order
λ	$\equiv$	wavelength
a	$\equiv$	spacing of lines or grooves
Θ_m	$\equiv$	angle of reflected energy of order m
Θ_i	$\equiv$	angle of incidence

A grating is blazed in order to concentrate maximum energy at an order other than m = 0 (Ref 17:69). The blaze wavelength (λ_b) is determined by

$$\lambda_b = \frac{2a\sin\Theta_b}{m} \qquad (19)$$

where Θ_b is the blaze angle. Because CO_2 and N_2O have many lasing transitions, the grating can be used to tune from one line to the next by adjusting the angle of incidence the laser beam makes with the grating. Since the grating disperses the various wavelengths, only one line will be reflected back onto itself, thus creating a laser cavity at a single wavelength.

-27-

Intra-Line Tuning

For some high resolution spectroscopy experiments, it is desired that a single laser line have a tunable linewidth much larger than the doppler linewidth. Abrams (Ref 12) has demonstrated a CO_2 waveguide laser tunable over 1200 MHz using a collision broadened system versus a 50 MHz linewidth available using doppler broadening. The homogeneous linewidth (full width half maximum (FWHM)) for a CO_2 laser is approximately represented by (Ref 2)

$$\Delta \nu = 7.58 \left[f_{CO_2} + 0.73 f_{N_2} + 0.64 f_{He} \right] P(300/T)^{1/2} \quad MHz \quad (20)$$

where f_x is the fraction of the gas x, P is the total pressure in torr, and T is the temperature of the gas. Also, in the absence of any mode selection device, the tuning range of the laser is limited by the free spectral range (c/2L) between two adjacent modes of the cavity.

A piezoelectric transducer (PZT) can be used to translate one of the reflectors in the cavity. When a ramp voltage is applied to the PZT, the reflector mounted in the PZT will translate along the axis of the resonator, thus changing the allowed wavelength of the cavity. Recall that a resonator (of length L) will support a wavelength λ according to

-28-

$$L = \frac{n\lambda}{2} \; ; \; n = 1, 2, 3 \ldots \qquad (21)$$

Therefore, as the length of the cavity is changed the wave-length will also have to change in order for lasing to occur. Since lasing lines have a finite linewidth according to Eq (20), it is possible to change the length of the resonator, by means of the PZT, to scan across the linewidth. Thus, intra-line tuning is achieved.

Losses

Within a laser system, losses are always present. In the following section, a qualitative look at some of the expected losses will be taken, as well as their causes. One loss mechanism has already been extensively discussed, coupling losses. As previously mentioned in this chapter, coupling losses occur because of a mismatch between mirror curvature, positioning, and size, and the guide aperture. A second mechanism for losses can involve a grating. One reason for losses in gratings is that they are not 100% efficient, therefore, some energy is lost through absorption and scat-tering. Another loss mechanism in gratings is the coupling between various orders. For example, if a grating is being used in the first order, it may also couple out some energy at the zero order. In some circumstances, it may be desir-

able to couple out the energy in this manner. If not, then the coupling between orders represents an undesired loss.

The temperature inside the waveguide (which acts as the discharge tube) can have many effects. First of all, an increase in the gas temperature can cause an increase in the population of the lower lasing level, thus reducing the population inversion. Secondly, an increase in the temperature can raise the pressure inside the guide, which could have a detrimental effect on the gain (Ref 2:19).

Finally, losses in the waveguide vary as function of the guide material. BeO (Beryllium Oxide) is reported (Ref 13:482) as being the best waveguide material at 10 μm because of its thermal conductivity and low waveguide losses. Other materials such as glass and alumina (Al_2O_3) have higher losses and lower thermal conductivity, but in some applications prove to be adequate in performance.

III   DESCRIPTION OF THE LASER

One of the major goals of the present thesis was to build a tunable CO_2 waveguide laser whose design and construction could be characterized by its overall simplicity. The laser's components were to be relatively inexpensive and readily available in the laboratory. Some components were chosen to match others that were available in the laboratory (i.e. the height of the cooling block was chosen to match the height of the mirror mounts). Many of the design criteria, as well as choice of materials, were selected so that the work of Gerlach and Amer (Ref 14) could be reproduced. They demonstrated that inter-line tuning was possible using their simple design; however, they had not determined the intra-line tuning range of a single lasing line - which is one of the primary objectives of the present thesis.

The chapter begins with a description of the waveguide tube assembly. The optimum resonator design is presented and variations from that design are discussed. Details of the gas and vacuum system are presented, as well as the electrical system. The chapter concludes with a descrip-tion of the diagnostic equipment (and set-ups) used throughout the experiment.

Waveguide Tube Assembly

(A photograph of the laser built for the present thesis appears below, in Fig. 10a.) An alumina tube having a 2.4 mm inner diameter and a 4.8 mm outer diameter served as both the discharge tube and the waveguide. Its length was 28 cm; this length was chosen in order to reproduce the results of Gerlach and Amer. The waveguide material, alumina, was selected because of its non-toxicity, adequate performance, and its inexpensive cost and availability in the laboratory.

Ordinary stainless steel Swagelok tees were attached to both ends of the tube. The Swagelok tees fulfilled three roles simultaneously; they acted as gas ports, electrodes, and Brewster angle window mounts (see Fig. 10b). The gas mixture entered one tee, flowed down the discharge tube, and exited the other tee. Electrodes were connected to the tees to provide a voltage drop across the discharge tube. Teflon ferrules were used in connecting the gas lines and the discharge tube to the Swagelok fittings, while stainless steel ferrules were between the Brewster window mountings and the Swagelok tees. Zinc Selenide (ZnSe) was used as the Brewster window material because of its ease of handling in the laboratory (vs. NaCl windows which require more care due to its hydroscopticity). The Brewster angle for ZnSe was calculated (Ref 15:245) to be
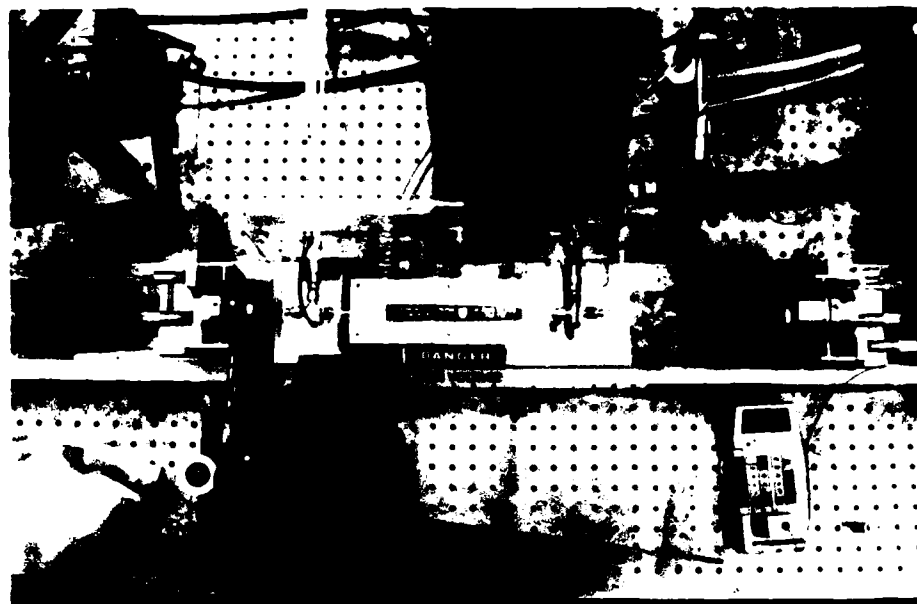
(a)

(b)

Figure 10.   a) Photograph of laser, b) close-up of multi-
              purpose Swagelok tees

67.4°. The windows were mounted such that they were facing up (see Fig. 10a), thus polarizing the output of the laser in the vertical direction (Ref 16:493).

The discharge tube assembly was placed into a round groove of a water-cooled aluminum block 9"x3"x2.28" (see Fig. 10a). Another grooved aluminum block 9"x3"x0.1875" was fastened down of top of the tube. Thermal joint compound was spread between the tube and the block to improve the thermal contact. Since the discharge tube is not directly cooled by the water, it is not necessary to make water-tight seals around the tube. The cooling block was mounted to a steel U-beam 120 cm long by four 1/4-20 screws. The U-beam provided both portability of the laser and served as an optical bench. Two mirror tracks, 15"x3-5/8"x0.05" were also bolted to the U-beam. Lansing mirror mounts were used and moved easily along the mirror tracks. The mirror mounts were held in position by means of an adjustable clamp (see Fig. 11). The clamp, which was screwed into the table, had a screw which could be turned such that the mirror mount was held tightly between the screw and the U-beam.

The cooling block and waveguide tube assembly were enclosed in a multi-purpose plexiglass shield. First and foremost, the enclosure protected the operator from the high voltage applied (up to 20kV) to the laser's discharge
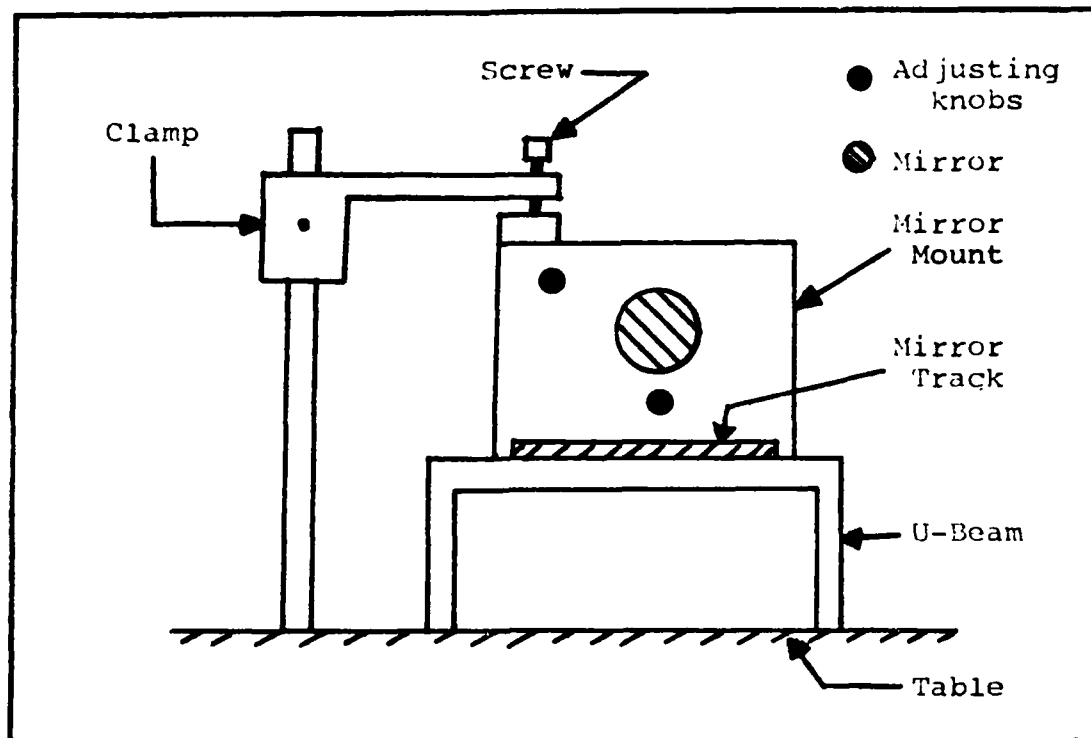
Figure 11. Mirror Position Clamps, End View

tube. Secondly, the shield protected the laser from acci-
dental damage (i.e. bumping the discharge tube or getting
fingerprints on the Brewster windows). Lastly, the shield
acted as a bulkhead and provided stress relief between the
water, gas, and electrical connections, and the waveguide
tube assembly (see Fig. 12). If the stress were not
relieved, there was a very good possibility that the tube
would have been broken because of the weight of the gas
(actually vacuum) line.

1. GND Lead Connector
2. GND Lead
3. HV Lead Shield
4. HV Lead
5. HV Bulkhead Connection
6. Gas Bulkhead Fittings
7. Gas Outlet Fittings
    (Vacuum Side)
8. Water Ports
9. Air Vents
10. U-beam
11. The Bulkhead
12. HV Coax
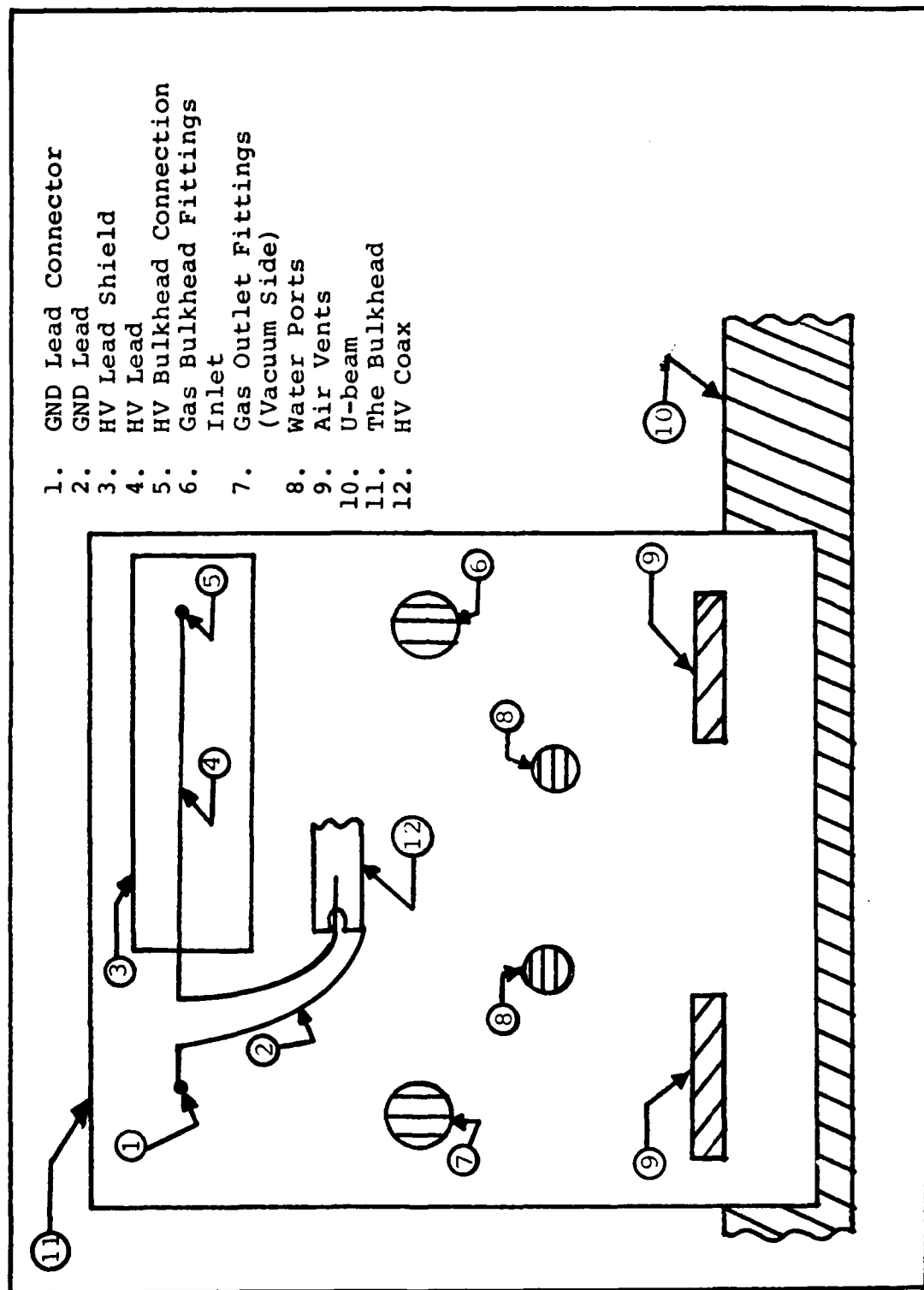
Figure 12. Stress Relieving Bulkhead

Resonator Design

The resonator consisted of three items: the
waveguide, a total reflector, and an output coupler. The
waveguide had an inner radius, a, equal to 1.2 mm. The
radius of the waveguide was a critical parameter in the
design of the resonator - the mirror curvature and spacing
are dependent on a. The case III configuration (see
Chapter II) was chosen because of its excellent transverse
mode discrimination even when large mirrors were used.
For case III,

$$\alpha = 2.415, \quad \beta = 0.5 \tag{22}$$

or

$$R = 2b, \quad z = b$$

where α and β are defined by Eq (15), R is the radius of
curvature of the mirror, z is the distance of the mirror
to the waveguide aperture and $b = \pi(.6435a)^2/\lambda_o$
(from Eqs (12) and (13)) and λ_o is the free space wave-
length of the laser. For $a = 1.2$ mm,

$$R = 35.3cm$$

and

$$z = 17.7 \text{ cm}$$

While it was desired to have 35 cm radius of curvature
mirrors, none were available in the laboratory. However,
some 25 cm optics were available and were used in the
experiment. Figure 6 shows that for R different than the
optimum R, the coupling losses increase. Specifically,
the losses are greater for a R smaller than the optimum R,
than the losses for a R larger than optimum. The coupling
loss for R/b = 1.4 (= 25/17.7) is approximately 11% (see
Fig. 6).

The original resonator consisted of two spherical
mirrors - one total reflector, and an output coupler with
a reflectivity of 95%. Later, output couplers with
reflectivities of 90% and 65% were also used.

Variations from the Spherical-Spherical Resonator

Throughout the experiment, variations from the
spherical-spherical resonator were made. A flat (R = ∞)
total reflector replaced the R = 25 cm total reflector in
order to develop alignment techniques, which were neces-
sary when a grating was used as the total reflector. The
goal of having a grating in the laser cavity was, of

-38-

course, to attempt inter-line and intra-line tuning. When
the flat or the grating was used, an AR coated germanium
lens was placed in front of the reflector in order to
increase the output power of the laser.

The grating had 150 grooves/mm and was blazed at
10.6 μm in the first order. Since the grating was used in
the Littrow orientation, the grating was mounted at 52° off
the normal (solved from the grating equation, (Ref 17).
The angular dispersion of the grating, was 81 Å/mrad. The
mounting holding the grating had 12° of angular movement,
enabling the grating to scan a wavelength region of 1.7 μm
- enough to scan from the R branch of the 9.4 μm band to
the P branch of the 10.4 μm band of CO_2.

The last variation of the waveguide resonator was the
addition of a piezoelectric translator (PZT). The output
coupler was mounted in the PZT. When a ramp voltage of
0 to -1.6kV was applied to PZT, it would expand linearly
from 0 to 12 μm. The PZT was driven by a sawtooth output
of an oscilloscope and amplified times ten such that the
voltage ramped between 0 and -1.2kV. This meant there was
an extension range of 9 μm instead of 12 μm. Since FSRs
are separated by an integral number of half-wavelengths
[P(20)]/2 = 5.3 μm), moving the output coupler 9 μm meant
that 1.7 FSRs (9 μm/5.3 μm) could be scanned.

Gas and Vacuum System

The gas used in the laser was mixed in a gas bottle at the laboratory's mixing station. The gas mixture contained 10% N_2, 20% CO_2 and 70% He; the same optimum gas mixture was used in the experiment of Gerlach and Amer (Ref 14). After the gas was mixed at the mixing station, it was spun on rollers to insure that the gas was thoroughly mixed. A diagram of the gas and vacuum system is presented in Figure 13. Quarter-inch plastic tubing connected the gas bottle to the needle and toggle valves. Two vacuum gauges measured the pressure in the gas line. A thermocouple (range, 1 to 1000 μm Hg) was used to measure the pressure when the gas line was evacuated (typically down to 15 μm torr). The second gauge, a mechanical gauge (range 1 to 800 torr), was used to measure the pressure of the gas when the laser was operating. Quarter-inch plastic tubing was also used to connect the needle valve to the gas bulkhead fitting, and from the bulkhead fitting to the 1/4" to 3/16" stainless steel Swagelok reducer. Gas flowed into the reducer, through the Swagelok tee, down the waveguide, and out the other Swagelok tee. The Brewster windows were cemented onto their mounts with Torr Seal, sealing the gas vacuum system from atmospheric air. The used gas exited the system through a valve which could be throttled to control the pressure in the waveguide. The vacuum pump was a rotating-vane pump capable of pumping 820,000 sccm.

1. Gas Bottle
2. Gas Regulator
3. Gas Flow Meter
4. Toggle Valve
5. Needle Valve
6. Thermocouple
7. Pressure Gauge
   (1-760 torr)
8. Bulkhead Fitting
9. 1/4" to 3/16" Connector
10. Swagelok tee
11. Waveguide
12. Vacuum Hose
13. Vacuum Valve
14. Vacuum Pump
15. 1/4" Tubing
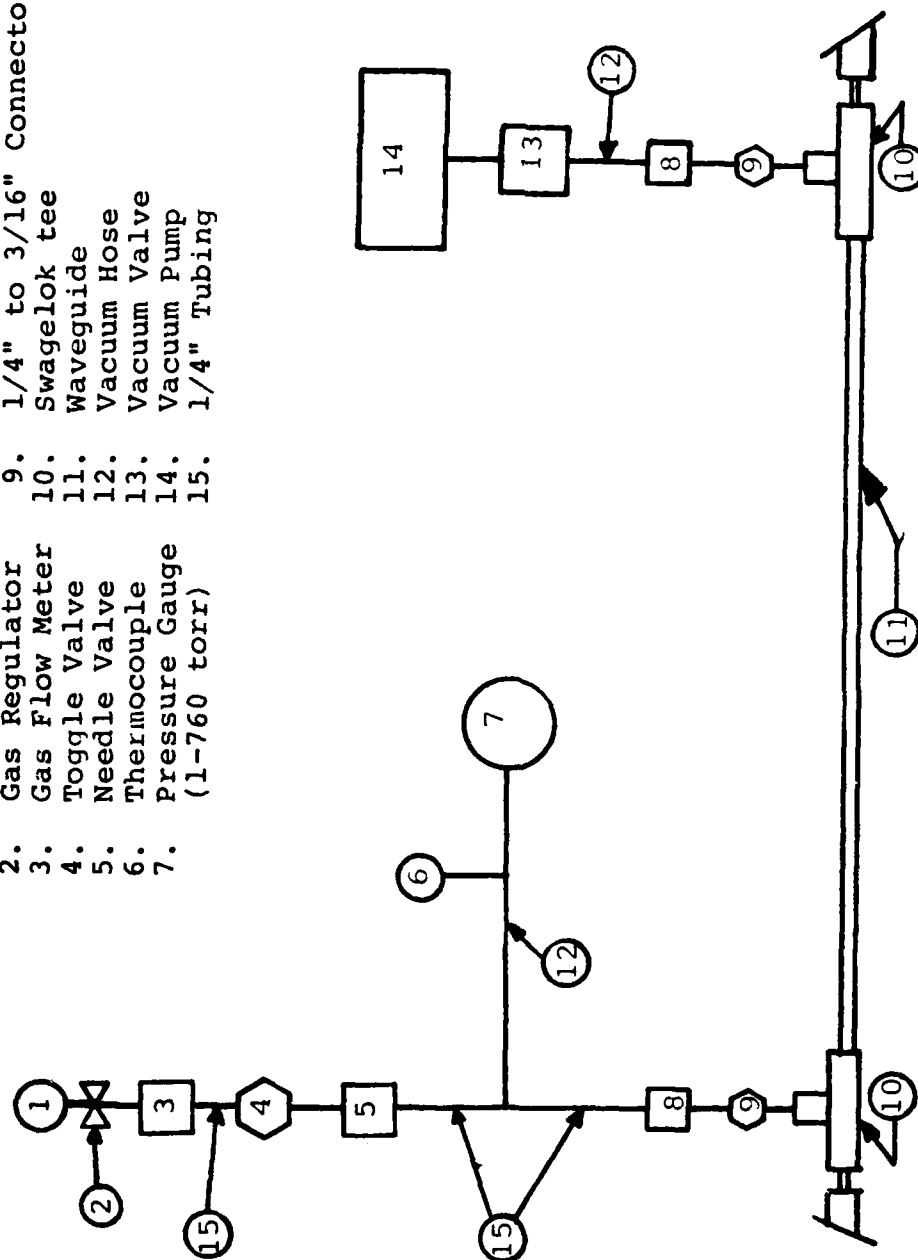
Figure 13. Gas and Vacuum Diagram

-41-

A flow meter was placed between the gas bottle and the
toggle valve to measure the flow of gas during laser
operation.

The Electrical System

The electrical system of the laser consisted of the
following: a 20kV/200mA Spellman DC power supply, a
ballast resistor, electrodes, and a discharge tube (see
Fig. 14). Breakdown voltages ranged from 10kV to 20kV
(dependent upon the pressure of the gas in the discharge
tube), while operating voltage varied from 8kV to 15kV.
The current ranged from 3mA to 15mA.

A ballast resistor was required to produce a stable
discharge in the discharge tube. The ballast resistor
($R = 400$ kΩ) also acted as a current limiting device. The
maximum current I_{max}, that could occur was

$$I_{max} = \frac{V_{s_{max}}}{R} = \frac{20,000}{400,000} = 50 \text{ mA}$$

where $V_{s_{max}}$ is the maximum supply voltage and R is the
ballast resistance. The ballast resistor was enclosed in
a plexiglass box to protect the operator from electrical
shock.

The electrodes were made of two parts: the Swagelok
tees previously mentioned, and two aluminum "c-clamps"

1. Power Supply   5. Bulkhead to electrode wires
2. High Voltage Coax   6. Discharge Tube
3. Ballast Resistor   7. Temperature Meter
4. Electrical Bulkhead   8. Electrodes
   Connection
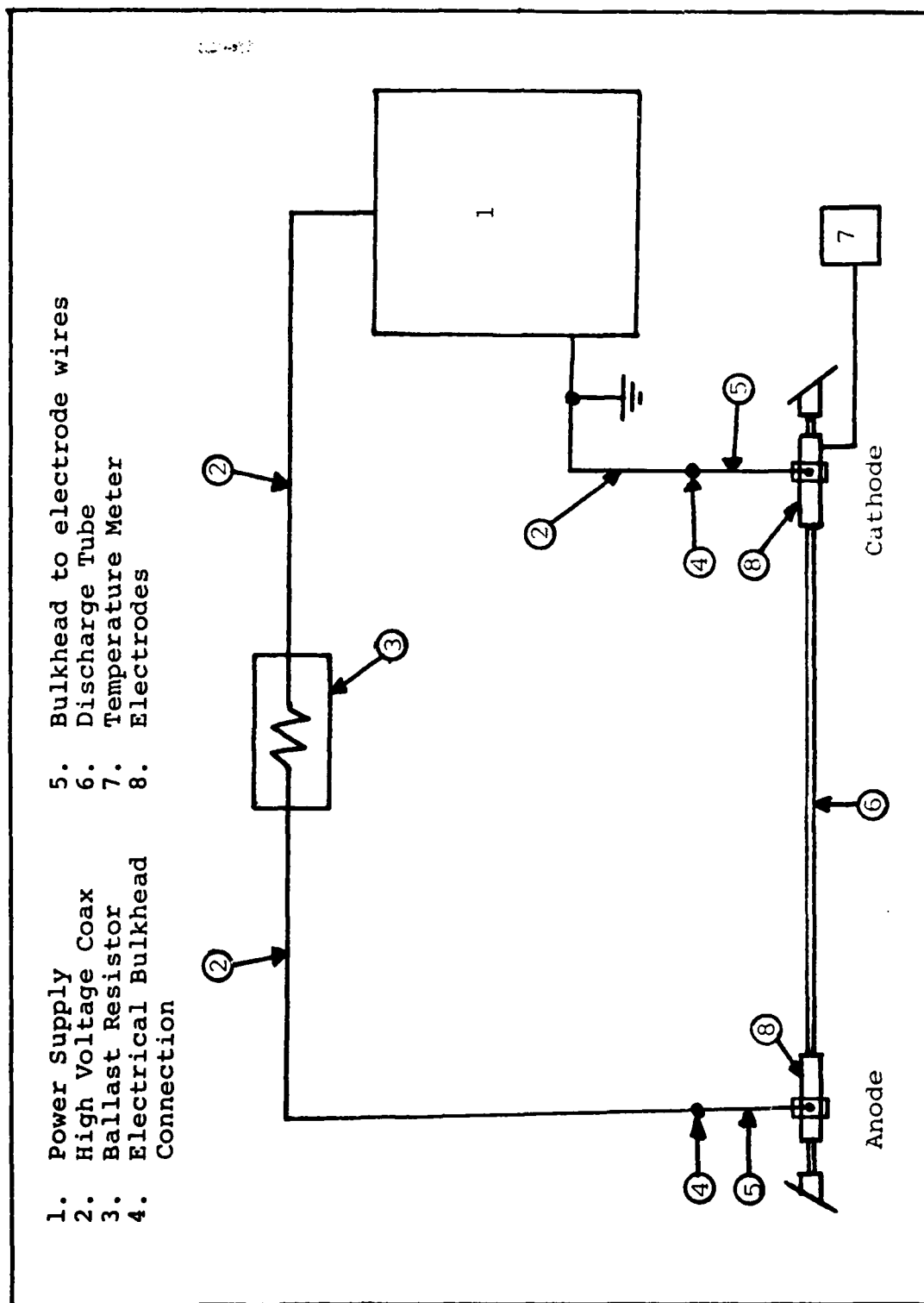
Figure 14. Electrical "Wiring" Diagram

(see Fig. 10). The c-clamps provided a means of electri-
cally connecting the Swagelok tees to the electrical
circuit. Wires ran from the bulkhead to screws on the
c-clamps; the c-clamps were tightened onto the tees using
screws that extended from the c-clamps and pressed against
the tees. When a potential difference was across the
electrode (hence, across the waveguide tube), a discharge
was formed in the tube.

A piece of Teflon was inserted between the anode (at
HV) and the cooling block (at GND) to prevent any arcing.
The distance, z_{bd}, between the anode and the position of
a grounded piece of equipment had to be at least

$$z_{bd} = \frac{V_s}{E_c} = \frac{20,000 \ V}{30,000 \ V/cm} = 0.67 \ cm$$

to prevent breakdown between them, where V_s is the supply
voltage and E_c is the critical electric field at which
breakdown occurs. The cathode was cooled by a small
electric fan which prevented the Torr-seal (used to cement
on the Brewster windows) from overheating.

Diagnostic Equipment

Throughout the present thesis, various diagnostic
equipment was used. There were three distinct phases in
the project, each requiring different sets of equipment.

The first stage was building a multi-line laser (i.e. no tuning elements were in the cavity). A thermopile detector was used to observe the initial lasing. Once the resonator was sufficiently aligned, other detectors - liquid crystal "paper", thermal imaging blocks (by Optical Engineering), and a thermocouple (power range - .01 W to 10 W) power meter - were used to observe the laser output. The thermal imaging blocks were especially convenient to use because both mode quality, as well as relative intensity of the laser beam, could be observed. A monochrometer was used to determine which lines were lasing.

The second phase of the experiment was to build an inter-line, tunable laser. A grating was used to achieve single-line lasing. Power measurements of the individual lasing lines were made by placing a movable beam steering mirror in front of the monochrometer (see Fig. 15), which was used to identify the lasing lines.

The final phase of the experiment was to build an intra-line tunable laser. A PZT was installed in the cavity in order to change the oscillation frequency of the laser output. The P(20) line of CO_2 (10.4 µm band) was scanned for intra-line tunability. As a ramp voltage (created by amplifying the sawtooth output of an oscillo-scope) was applied to the PZT, the frequency of the laser beam was scanned. The beam was split by a piece of ZnSe
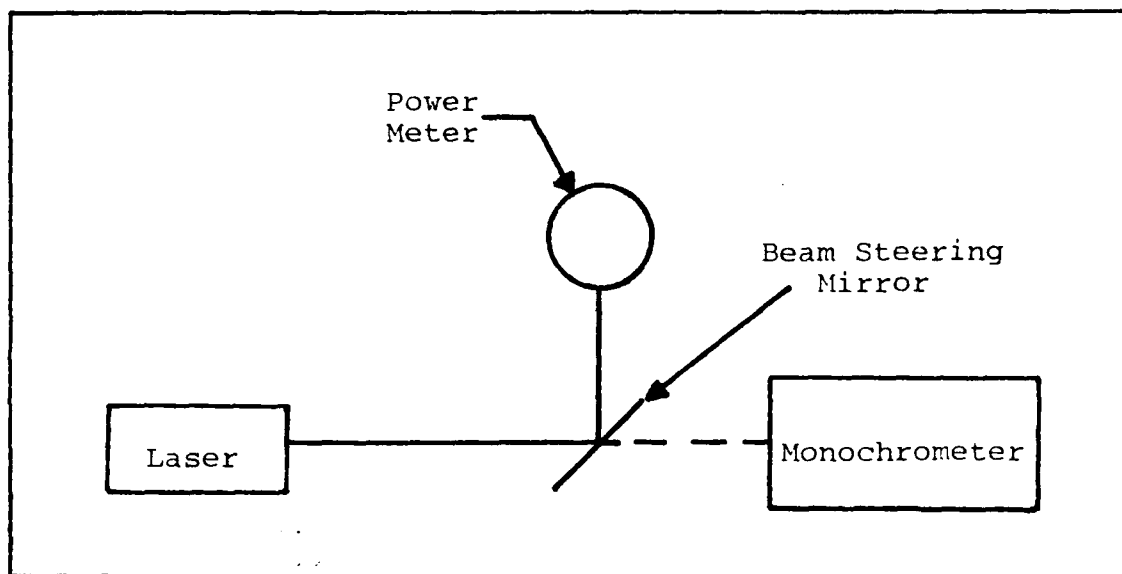
Figure 15.   Diagnostic Equipment for Inter-line Tuning

(see Fig. 16); most of the beam continued into the mono-

chrometer, while the reflected part of the beam passed

through a chopper and a gas absorption cell before entering

a fast detector (i.e. a pyro-electric or a HgCdTe).   The

absorption cell was a White-type cell whose pathlength was

adjustable.   The pathlength could be varied from 0.75 m to

20.25 m.   The output of the detector was fed into an AC

voltmeter which had a chart recorder output.   This output

was simultan- eously fed to the y axis of an x-y chart

recorder and to an oscilloscope.   The ramp voltage of the

oscilloscope was used to drive the x-axis of the chart

recorder.
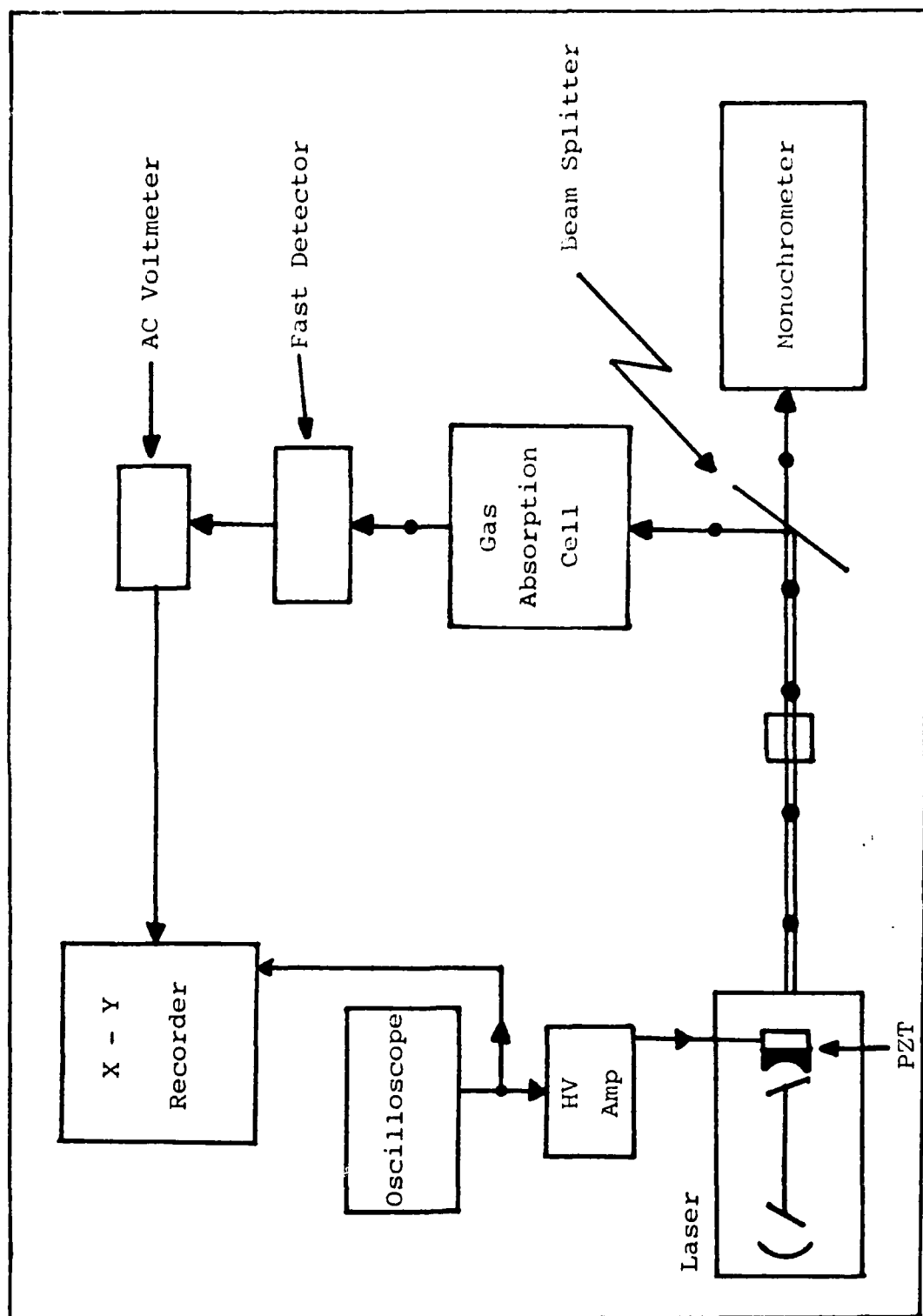
Figure 16. Set up for Intra-line Tuning Experiment

IV RESULTS

Throughout the thesis, three major areas of interest were investigated. The first area of investigation involved the waveguide laser in a multi-line configuration; i.e. no tuning element was used in the cavity. Both CO_2 and N_2O gas mixes were used as lasing media. Secondly, the inter-line tuning characteristics of the waveguide laser were investigated using a grating as the total reflector. Lasing occurred only with the CO_2 gas mix as the lasing medium; the N_2O mix did not lase in the single-line configuration. Thirdly, a PZT was used to observe intra-line tuning on the P(20) line of CO_2. The chapter concludes with a discussion of some significant problems encountered in the laboratory.

Multi-line Configuration

In the multi-line configuration, the waveguide resonator consisted of the waveguide, and two spherical mirrors - one was a total reflector, the other, a partial reflector. Two gas mixes, CO_2 and N_2O, were used as the lasing media. The laser was optimized for maximum power as a function of the discharge current, gas pressure, mirror position, and the fraction of every coupled out through the partial reflector. The results of the CO_2 laser are presented first.

The maximum laser power achieved in the multi-line configuration was 7.5 W. The discharge current was 14 mA, the discharge voltage, 8.1 kV, and the mirrors were 27.5 cm from the end of the waveguide. The gas mix contained 10% N_2, 20% CO_2, and 70% He. The ratio of gases in the gas mixture remained the same throughout the experiments.

Discharge currents in the laser were limited for two reasons. First of all, the lower limit of the current, where lasing occurred, was that current which was enough to sustain a stable discharge in the tube. While this minimum current changed with the gas pressure in the laser, it was generally found that 3 or 4 mA was necessary to produce a stable discharge where lasing could occur. Secondly, the upper limit of the discharge current was that current which caused lasing to cease. This upper current also varied with the pressure in the laser. Generally, this occurred for currents larger than 15 mA.

Typically currents between 5 mA and 7 mA were found to be optimum to achieve maximum power out. Increases or decreases in the discharge current generally caused a decrease in the output of the laser; however, there were times when the current was increased from 6 to 10 mA with little change in the output power of the laser. This indicated that saturation was occurring. Therefore, the

output coupler was changed from a 95% reflector to a 90%
reflector so that more laser energy could be extracted
from the cavity. Thus, a peak output power was obtained
for a discharge current of approximately 7 mA.

Pressure Variations

The laser was operated at gas inlet pressures ranging
from 25 torr to 162 torr. About 50 mW was detected at the
latter pressure. The optimum "hot" pressure of the gas
was found to be 87 torr, which corresponded to a "cold"
pressure of 70 torr. "Cold" pressure refers to that pres-
sure measured when the discharge was not on. When the
discharge was turned on, the temperature of the gas in-
creased and caused the pressure to rise to its "hot" value
in about 30 seconds. The "hot" pressure was, on the
average, about 23 percent greater than the "cold" pressure.
Since the "hot" pressure was the steady state pressure
(i.e. the final pressure), only the "hot" pressure will be
mentioned hereafter.

The gas pressure was measured only at the inlet gas
port. Since it was desired to know the average pressure
in the discharge tube, the pressure drop across the tube
was calculated using the following equation (Ref 19):

$$P_2 = \left[P_1^2 - \frac{2QL\eta}{(3.27 \times 10^{-2})D^4} \right]^{1/2} \quad \text{torr} \qquad (23)$$

where P_2 is the outlet pressure, P_1 is the inlet pressure in torr, Q is the gas flow in $1 \cdot torr \cdot sec^{-1}$, L is the length of the tube in cm, D is the diameter of the tube in cm, and for this particular gas mix $\eta = 1.75 \times 10^{-4}$ torr sec. Thus for an inlet pressure of 87 torr, the average pressure is 79 torr for a Q = 21.

In Figure 17, a family of curves is presented which shows the output power as a function of gas pressure and mirror position. It can be seen that an inlet pressure of about 87 torr does indeed provide maximum power out. The maximum output power occurred when the mirror position (M.P.) was at a distance slightly greater than the radius of curvature (R) away from the guide (M.P. = 27.5 cm, R = 25 cm, see Fig. 18). This is consistent with the results of Degnan (Ref 2) and Gerlach and Amer (Ref 14). The maximum is thought to occur because the higher order waveguide modes couple together with the fundamental mode when the mirror position is approximately equal to R, thus producing greater output power.

There was a relative maximum in the output when the mirrors were 18.5 cm from the ends of the waveguide. Since the waveguide laser was designed for Degnan's case III (see Chapter II), we would expect a relative maximum to occur when the mirrors were a distance equal to one-half the radius of curvature away from the guide. For
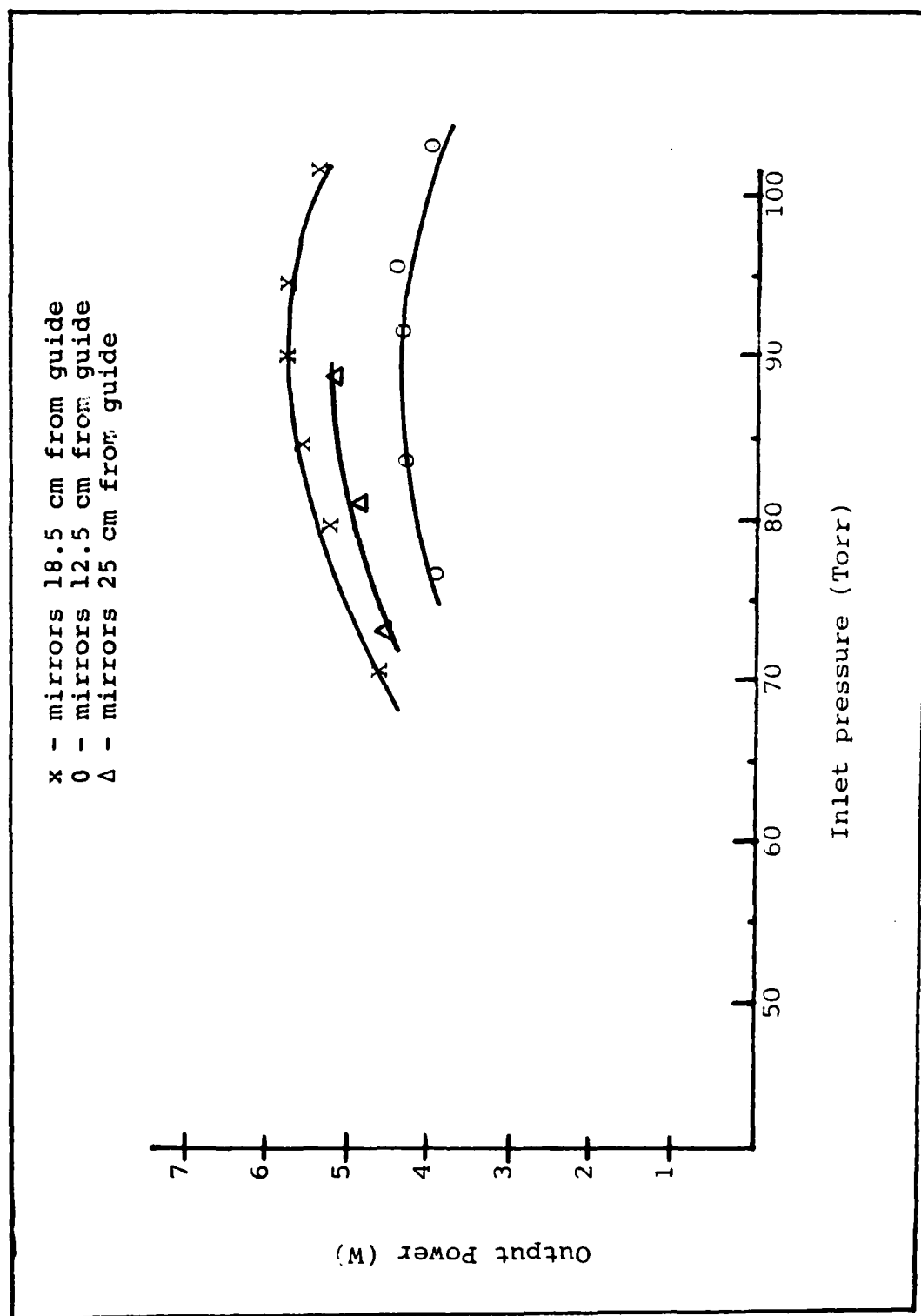
Figure 17. Output Power vs. Gas Pressure and Mirror Position

x — mirrors 18.5 cm from guide
0 — mirrors 12.5 cm from guide
Δ — mirrors 25 cm from guide

Inlet pressure (Torr)
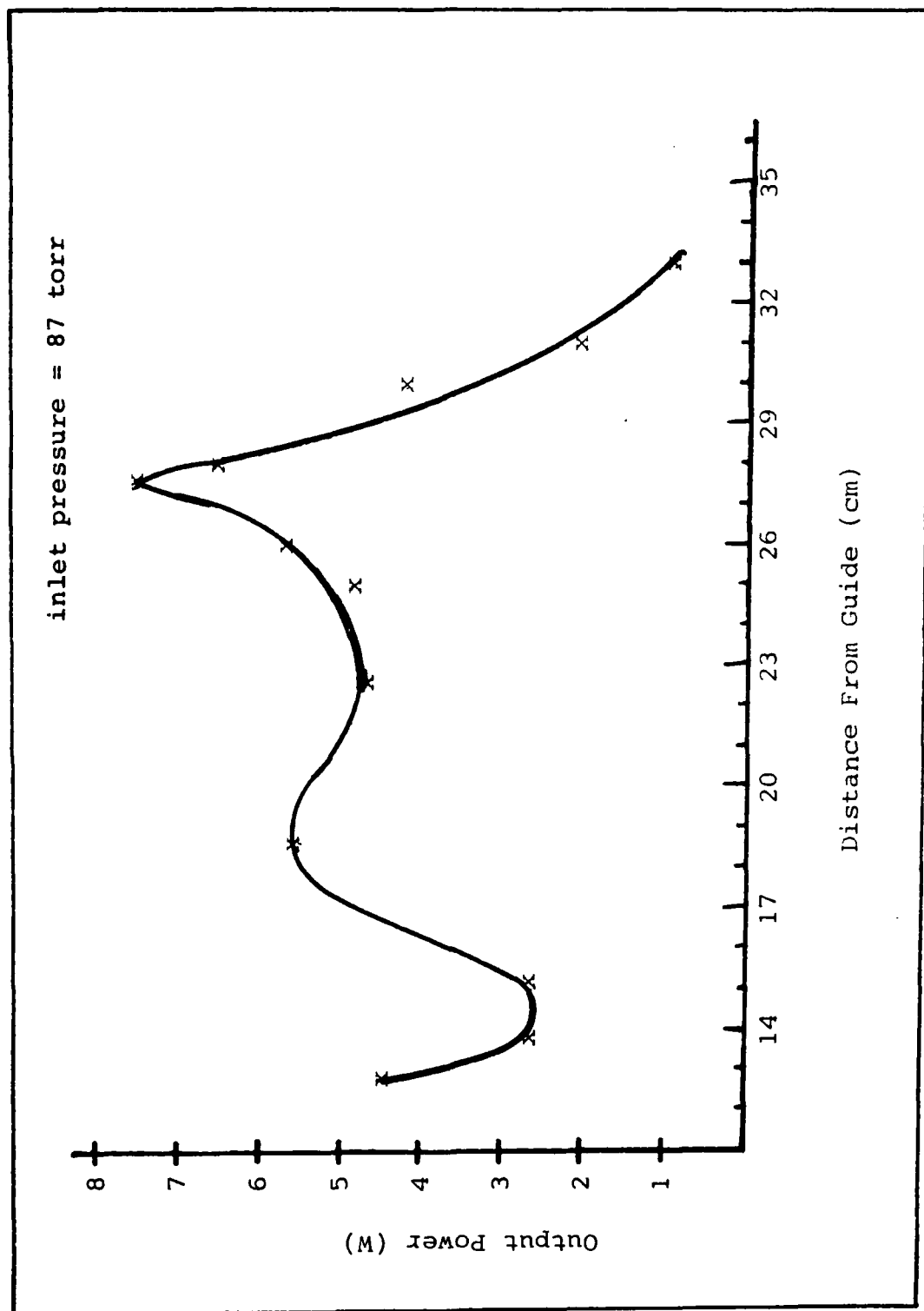
Output Power (W)

Figure 18. Output Power vs. Mirror Position (Constant Pressure)

optimum mirrors (R = 35.4 cm), this would occur near 17.5 cm. For the mirrors used (R = 25 cm), one would expect a relative maximum near 12.5 cm. One might expect one of the two above maxima to occur, but can both be expected, as is indicated by the data? The answer is probably yes.

The maximum of 12.5 cm may be expected because the coupling losses are near a minimum when the mirror is half the radius of curvature from the guide. Therefore, the output power will be greater. We know from theory (Ref 2) that a low coupling loss exists for an optimum cavity for the present waveguide near 18 cm. If the present mirrors matched the optimum mirrors we would definitely see a (relative) maximum near 18 cm. However, there is a mis-match between the phasefront curvature of the laser beam and the present mirror curvature, but the resulting losses may be small enough to allow the maximum (near 18 cm) that is seen in Figure 18.

Output Coupler Variations

Only a limited number of output couplers were avail-able in the laboratory, consequently, variations in output couplers were limited. The maximum output power, 7.5 W power was achieved with a 95% reflector while a maximum of 7.2 W was obtained using a 90% reflector. Both mirrors mentioned above had a radius of curvature, R = 25 cm.

A flat 65% reflector was placed near the end of the waveguide (10.8 cm away) and a maximum output of 6.0 W was achieved.

A comparison of the output power as a function of the output couplers may be somewhat misleading. Problems with Brewster window damage (see page 71 for details) were prevalent during the early stages of the experiment. Consequently, later data cannot be accurately compared with earlier data. The 7.5 W output was achieved during the latter part of experiment after much of the window problems were solved.

In general (at least in the early portions of the experiment), the 90% reflector produced greater lasing power than the other output couplers. Since the 65% reflector gave results nearly as good as the 90% reflector, one would expect a maximum output by using a reflector between the two. Other experimental results (Ref 14) suggest that an 84% reflector should be used to obtain maximum laser power, which is in ballpark agreement of the present results.

The N_2O Multi-line Laser

The multi-line N_2O waveguide laser achieved a maximum laser output of 825 mW with an inlet pressure of 55 torr and at a discharge current and voltages of 4.8 mA and 8.7 kV respectively. The gas mixture (premixed) was a

9.9/9.9/80.3 ratio of $N_2O/N_2/He$. Any deviations in the discharge current or inlet pressure resulted in a decrease in the output power. Other results (Ref 14) have produced output powers nearly twice as large. It is suspected that the gas mix used in the present thesis was not an optimum mix. Gerlach and Amer (Ref 14) reported a mix of 13% N_2O, 16% CO, 20% N_2, and 51% He. Time limitations in the laboratory did not permit variations in the present gas mixture in order to optimize the N_2O laser.

A monochrometer was used to view what line or lines the N_2O was lasing on. Only lines in the P branch of the 10.6 μm band were observed. The P(21) line was the dominant line and the laser tended to lase on that particular line more than any other. Other lines, P(13) through P(29), were induced to lase by intentionally causing small vibrations in the mirror mounts. While such a technique may be considered somewhat crude, it did reveal what lines could be expected to lase in a single line configuration (i.e. with a grating intra-cavity). The induced lasing lines lased only for a moment before returning to a stable line – generally either the P(19), P(20), or P(21) line.

Inter-line Tuning

The cavity for single line operation consisted of the waveguide, a 95% spherical reflector (R = 25 cm), an AR

coated germanium lens (F = 6.4 cm), and a grating. The lens was used to collimate the laser beam onto the grating and to increase the output power of the laser. The optimum focal length for the lens would be about 35 cm in order to produce the maximum power out and it would be positioned one focal length from the end of the waveguide. Since the only lens that was available had a focal length of 6.4 cm, it was placed as close as possible to the end of the guide (physical limitations of the system, both electrical and mechanical, prevented the lens and grating from being any closer than 12 cm away).

Lessons learned from the multi-line configuration were very valuable to the operation of the laser in the single line mode. The spherical mirror remained 27.5 cm from the guide to provide maximum power. The inlet pressure and discharge current also remained at their optimum values of 87 torr and approximately 7 mA respectively.

Lasing occurred on 50 different lines of the P and R branches of the 10.4 μm and 9.4 μm bands - P(6) to P(42) and R(6) to R(38) in 10.4 μm band, and P(14) to P(30) and R(16) to R(24) in the 9.4 μm band. The maximum power achieved in single line operation was 2.2 W, P(20), at an inlet pressure of 86 torr, discharge current of 7.5 mA and discharge voltage of 10.2 kV. From one day to the next, the output power could vary as much as 15 or 20 percent.

-57-

This was largely a result of spots (damage) on the brew-ster windows. As the resonator was tuned and realigned, the laser beam could wander onto one of the spots, which then caused a decrease in the output power. Aligning the resonator so that the laser beam did not pass through any spots was always a hit or miss operation.

The output power was measured as a function of the lasing line, the flow rate of the gas, and as a function of the output coupler (partial reflector). Table I shows the output power vs. the individual lasing and the power vs. the output coupler. It can be seen that the P(20) line is the strongest lasing line and that the power decreases as you move farther away from the dominant line. The same decrease in power is evident in the R branch as well. The 90% reflector produced slightly higher output power on the central lines of a branch, but the power died out quicker as a function of lasing line which resulted in fewer lines lasing. Therefore, if the goal is to achieve maximum inter-line tunability, and you are willing to sacrifice laser power to do so, then the 95% reflector is superior. The output power was found to be fairly inde-pendent of the gas flow rate for the range 750 sccm to 1750 sccm (see Table II) at a constant inlet pressure of approximately 86 torr.

Table I

Output Power vs. Lasing Line
and Partial Reflector

Lasing	Power Out (W)	
Line	95% Mirror	90% Mirror
P(8)	0.15	–
P(12)	0.65	0.37
P(16)	1.00	–
P(18)	1.50	–
P(20)	1.55	1.57
P(22)	1.10 *	–
P(28)	1.20	–
R(8)	0.47	–
R(10)	–	0.16
R(14)	1.20	–
R(16)	0.80 *	1.37
R(18)	0.85 *	–
R(20)	1.25	–
R(22)	–	1.27
R(24)	1.15	–
R(28)	1.00	–
R(30)	–	0.70
R(32)	0.80	–
R(36)	0.27	–

* These powers probably reduced because
of Brewster window damage.

Table II

Output Power vs. Gas Flow Rate

Gas Flow Rate	Power Out (W)
750 sccm	1.55 W
1000	1.50
1300	1.50
1500	1.43
1560	1.75
1620	1.50
1680	1.40
1750	1.40

Inter-line Tuning with N_2O

Attempts to lase with N_2O in the single line con-
figuration were not successful; there are at least two
probable causes for the failure. First, the premixed gas
did not contain an optimum mixture as explained earlier.
The second cause may have been the mirrors. Since the
mirrors did not produce a low coupling loss between the
guide and the mirrors (R = 25 cm, not the optimum 35 cm),
the higher than optimum losses, combined with the poor gas
mixture, may have prevented lasing. However, Gerlach and
Amer (Ref 14) did not report success either despite using
what they considered to be an optimum mix.

Intra-Line Tuning

The cavity for intra-line tuning was the same as the
inter-line configuration with one addition; a piezoelectric
transducer (PZT) was used to hold the output mirror. When
a ramp voltage of 0 to -1.2 kV was applied to the PZT, it
extended linearly into 9 μm. Since the length of a reson-
ator is of an integral number of half wavelengths, 1.7
FSR's can be scanned using the PZT ($\lambda/2$ = 5.3 μm, there-
fore the number of FSR = 9/5.3 = 1.7).

In the following discussion, the intra-line tuning
range will be presented; its limitations as well as its
dependency on the pressure of the lasing medium will also
be discussed. The lineshape of the tuned line, including

the causes for the lineshape, and means of verification

that tuning across the FSR occurred, are also presented.

The P(20) line, which was scanned using the PZT, had a

tunable linewidth of 215 MHz. This linewidth was limited

by the 224 MHz FSR of the cavity (L = 67 cm). The line-

width was also limited by the pressure of the gas in the

discharge tube. From Eq (20) it can be found that the

linewidth is directly proprtioned to the gas pressure

$$\Delta \nu \; = \; 5.465P \qquad MHz \qquad\qquad (24)$$

where P is the pressure in Torr. In order to get the

maximum tuning possible, set $\Delta \nu$ = 224 MHz and solve for

the maximum pressure, P_{max}

$$P_{max} \; = \; \frac{\Delta \nu max}{5.464} \; = \; 41 \; torr \qquad\qquad (25)$$

In Figure 19, the pressure dependence of the tunable

linewidth can easily be seen. The solid curve is a

recording of the output power for a laser pressure of 38

torr, while the dotted curve was at 27 torr. Because the

pressure is higher for the solid curve, it has a wider

linewidth in accordance with Eq (24). The linewidths can

also be estimated from these curves. Because the FSR of

the cavity is known (c/2L) to be 224 MHz, the frequency

scale of Figure 19 can be calibrated accordingly; the FSR
is the distance between the two nulls (or two maxima).
Now that the scale is calibrated, the linewidths can be
measured. For the solid line (P = 38 torr), Δv_{meas} = 203
MHz and from Eq (24) Δv_{calc} = 207 MHz. For the dotted
curve (P = 27 Torr), Δv_{meas} = 142 MHz and Δv_{calc} = 147
MHz. Both of the measured results are in very good
agreement with the calculated values.

Lineshape

It was found that very slow sweep speeds of the PZT
(up to 50 sec to scan the 1.7 FSRs) were possible with
little adverse effects on the lineshape. While a sweep
time, t_s, of 50 sec did allow for a small amount of
jitter in the output power, the slope of the overall line
profile was not affected; whereas, a sweep time of 5 sec
resulted in a smooth output power curve, yet the slope of
the line profile was greatly distorted (see Fig. 20). A
small amount of jitter, due to mechanical instabilities at
slow sweep speeds, in the output power is acceptable
because tunability, not smooth output power, is the desired
goal. (Note - The curves in Figure 20 are the results of
the tuned laser line passing through a gas absorption
cell; therefore, the lineshapes are accordingly different.
The profile of the t_s = 5 sec, however, remains

P = 38 torr

P = 27 torr

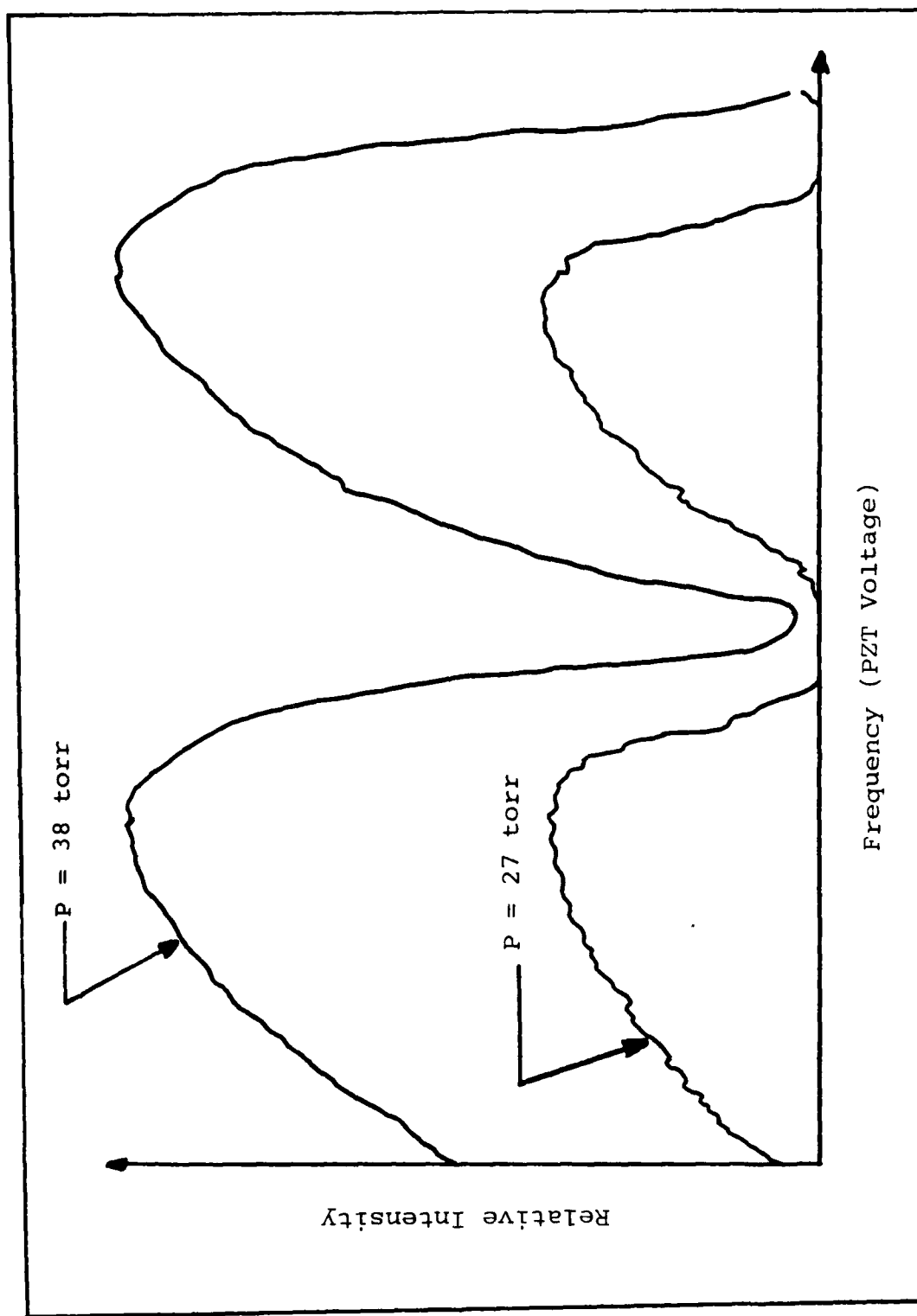Relative Intensity

Frequency (PZT Voltage)

Figure 19. Intra-line Tuning vs. Gas Pressure in Laser

distorted. Results of the gas absorption cell will be
presented after the next section.)

Returning to Figure 19 (the solid curve), it can be
seen that the curves are asymmetric. Others (Ref 13) have
reported similar asymmetric lineshapes. The causes for
the asymmetry are not yet understood, however, one
possible contributing factor is presented. As the laser
power began to drop (a function of the PZT voltage), a
transverse lasing mode was observed. It appeared to be
similar to a TEM_{01} mode of standard gas lasers. The
presence of this transverse mode may have extended the
peak lasing of the cavity, thus helping to create the
asymmetric lineshape.

Gas Absorption Cell Experiment

A gas absoption cell was used to verify (1) that tuning
across the P(20) line was occurring, and (2) that the dis-
tance between minima in the power curves actually repre-
sented the free spectral range. The gas absorption cell
could either be evacuated, or filled with a particular gas.
When the cell was evacuated, the laser beam passed through
the cell with no absorption taking place, which is how the
curves of Figure 19 were created. When pure CO_2 was
added to the gas cell, it caused absorption to occur. Both
the peak absorption and the width of the absorption were
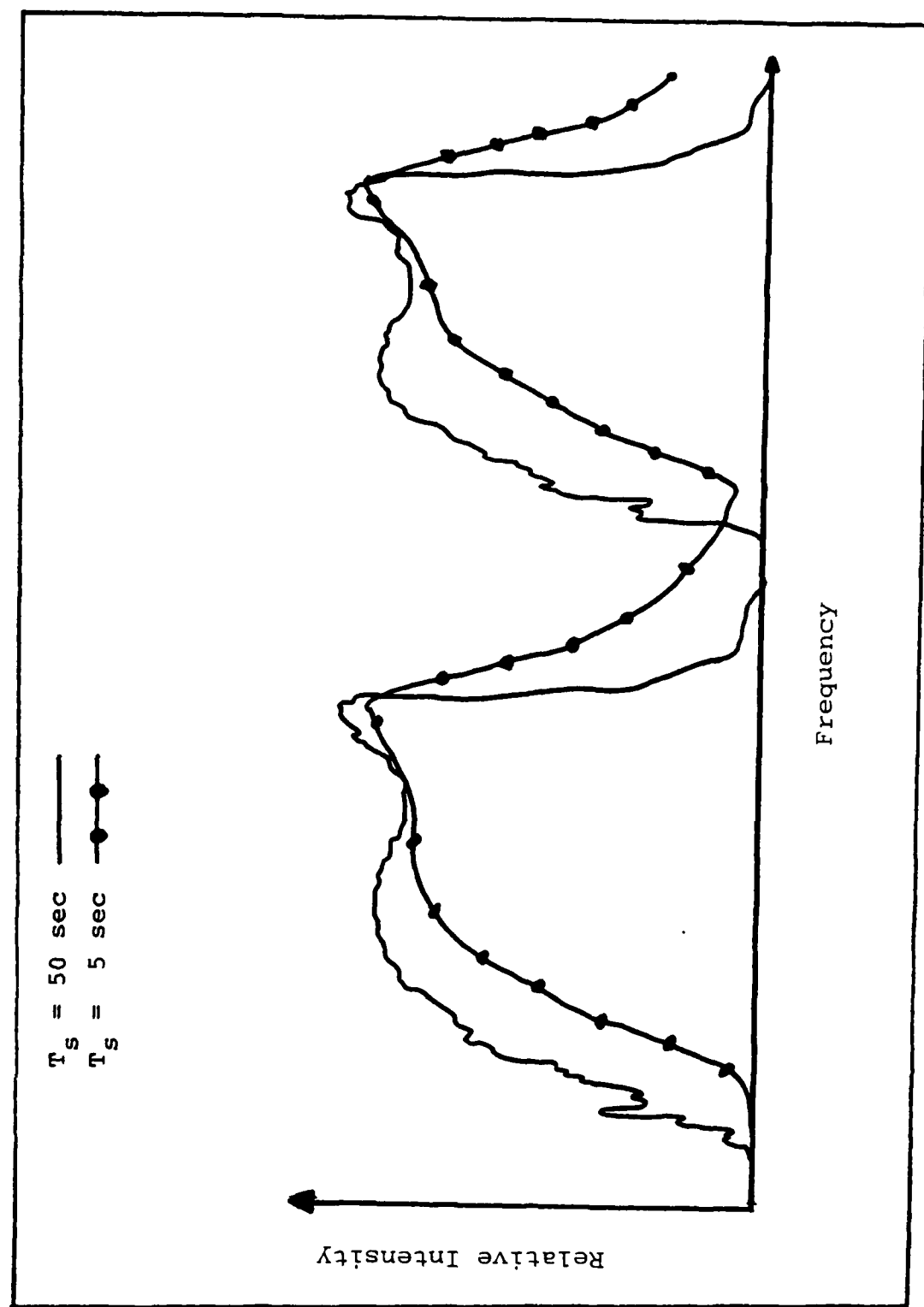dependent upon the CO_2 pressure in the gas cell.

-64-

Figure 20. Absorption Lineshape vs. Sweep Speed

Figure 21 illustrates the effect of varying the pressure of the CO_2 in the gas cell. For the solid curve, the cell was evacuated, hence, no absorption. However, when 3.7 torr of CO_2 was added to the cell, the absorption as a function of frequency became very apparent (dashed curve, Fig. 21). As more CO_2 was added to the cell, the absorption increased. Since the absorption increased, then decreased, and since it is known that absorption is a function of frequency, it can safely be stated that the change in absorption was caused by a change in the frequency of the laser beam. Thus, we have verification of intra-line tuning.

The peak absorption can be calculated by using Beer's Law

$$I = I_o \, e^{-kxp} \qquad (26)$$

where I_o is the intensity of the curve without absorption, I is the intensity with absorption, k is the absorption coefficient, x is the path length in the gas cell in cm, and p is the pressure in atm. The peak absorption coefficient for a cell pressure, P_c = 3.7 torr (in the Voigt regime, Refs 20,21,22)

$$k_o = 0.1885 \quad (cm\text{-}atm)^{-1} \qquad (27)$$
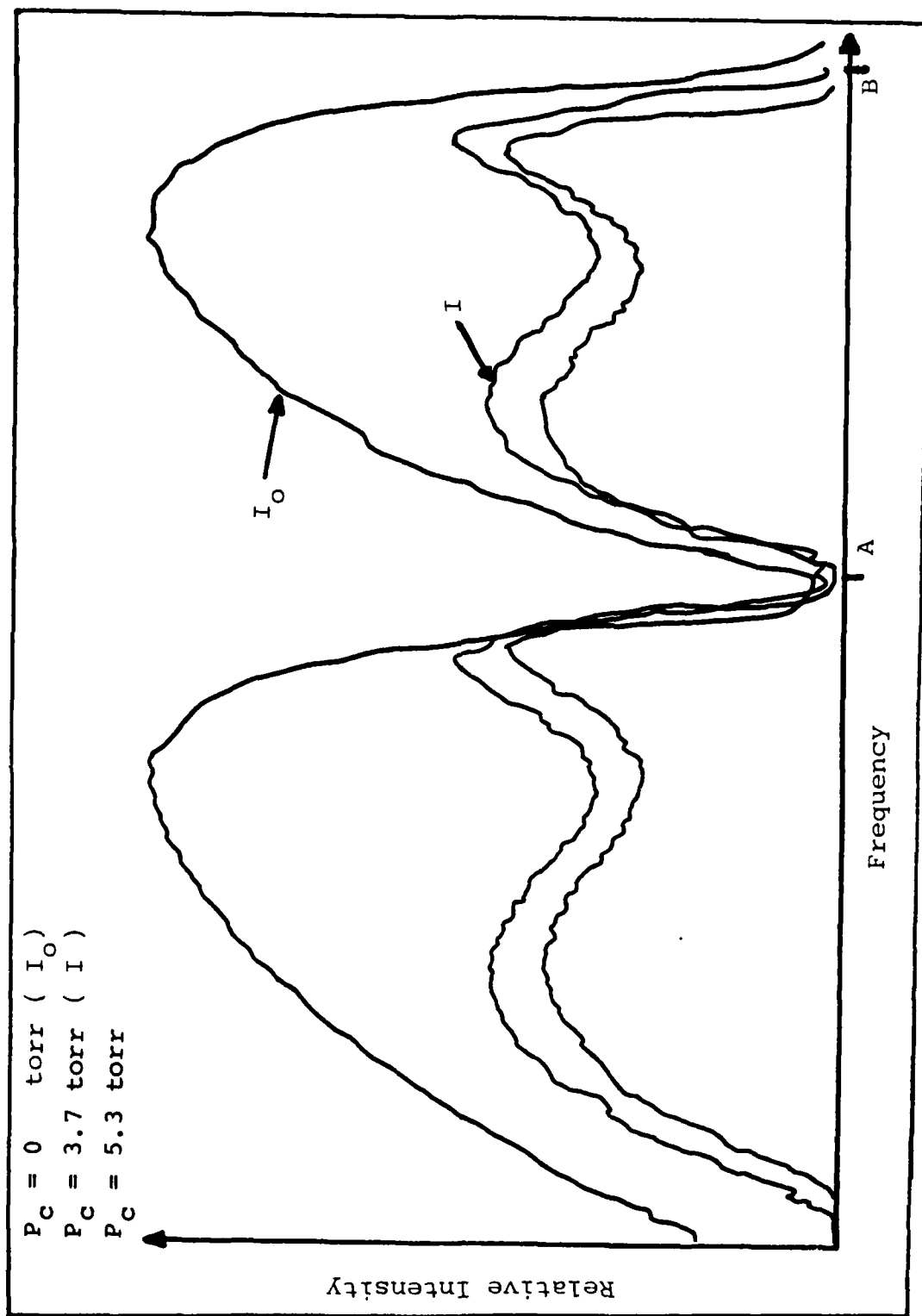
Figure 21. Absorption vs. CO_2 Cell Pressure

Therefore the peak absorption

$$(I/I_o)_{calc} = e^{-kpx} \qquad (28)$$
$$= 35.6\%,$$

for a path length of 1125 cm. The measured peak absorption, $(I/I_o)_{meas}$, for the dashed curve (P_c = 3.7 torr) of Figure 21 is

$$\left(\frac{I}{I_o}\right)_{meas} = 35.9\%$$

Once again, there is very good agreement between the experimental results and theoretical calculations.

We have already seen that minima of the power curves mark the FSR of the laser. The FSR can be verified by comparing the calculated and measured Voigt absorption widths (FWHM) as a fraction of the full width of the power minima. The Voigt width (FWHM) $\Delta\nu_v$ can be approximated as (Ref 23:1384)

$$\Delta\nu_v = b_c + (b_c^2 + 4b_D^2)^{1/2} \quad MHz \qquad (29)$$

where b_c is the collision broadened halfwidth at half MAX and b_D is the doppler halfwidth of CO_2 at half MAX, both in MHz. For a pressure of 3.7 torr, b_c = 14.9 MHz and b_D = 26.4 MHz. Therefore

$$\Delta\nu_V = 70 \text{ MHz} \qquad (30)$$

To find the experimental FWHM, it is necessary to begin with a form of Beer's Law

$$\frac{I}{I_o} = e^{-kpx} \qquad (31)$$

After taking the natural log of both sides, we find that

$$kpx = - \ln (I/I_o) \qquad (32)$$

The Voigt absorption profile is directly proportioned to the product kpx. Therefore, the FWHM of the plot of $-\ln(I/I_o)$ yields the Voigt width. The absorption profile of the dashed (I) and solid (I_o) curves of Figure 21 is plotted in Figure 22. The marks a and b in Figures 21 and 22, represent the same frequency range. If we assume the measured FWHM is equal to the calculated value (70 MHz), then the frequency range a → b would be approximately (2.4) x 70 MHz = 170 MHz. If we assume that the frequency range a → b is the FSR = 224 MHz then the measured Voigt width would be equal to

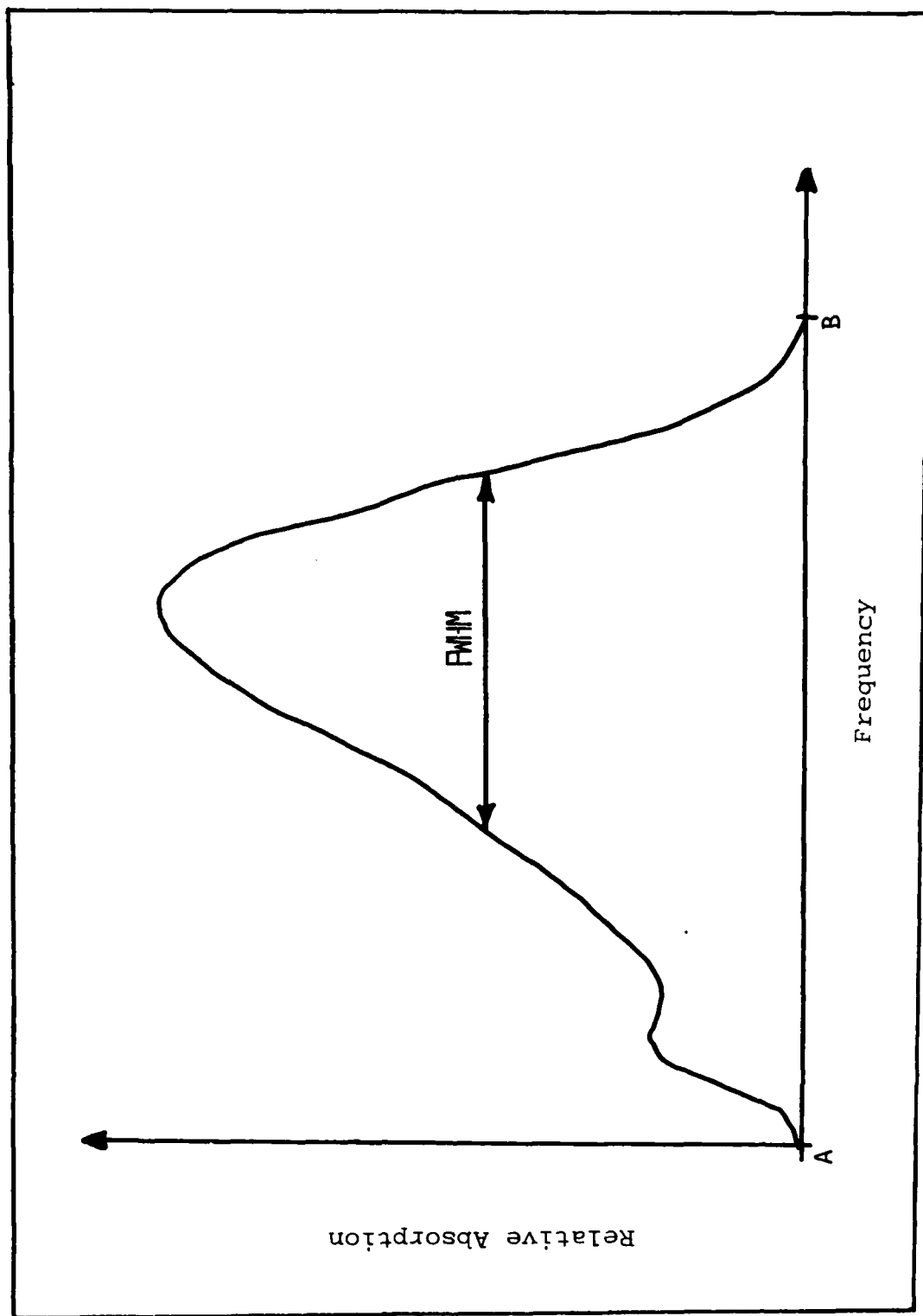$$(\Delta\nu_V)_{meas} = \frac{224}{24} = 93 \text{ MHz} \qquad (33)$$

Figure 22. The Voigt Absorption Profile

Since the measured Voigt width and the calculated Voigt width are in ballpark agreement, it is safe to assume that the frequency range a → b does, in fact, represent the FSR of the laser.

Finally it is noted that the FSR, and hence the maximum intra-line tunability, was limited by the length of the resonator. Therefore, if it is desired to have greater tunability, a smaller cavity must be designed. In order to make a shorter cavity, a waveguide tube with a smaller inner diameter must be used. The smaller diameter permits the use of smaller radius of curvature mirrors, which can be placed closer to the end of the waveguide. A 1.6 mm i.d. alumina tube is presently in the laboratory and it should be possible to build a resonator less than 30 cm long - which would give a tuning range of approximately 500 MHz.

Problems

During the operation of the laser, a few noteworthy problems were encountered. In this section, four problem areas will be discussed: Brewster window damage, detector response time, Brewster window reflections, and the transfer of vibrations through the mirror mounts. The biggest problem that was encountered was damage to the Brewster windows. Dark, burn-like spots appeared on both

the anode (gas inlet port) window and the cathode (gas outlet port) window. Once, the damage was severe enough to cause lasing to cease, and new windows had to be put on the tube. Since the damage occurred on both windows, the direction of the flowing gas can be ruled out as a cause for the spots. It was found that the windows could be cleaned using ethanol and gently rubbing with a Q-tip.

It is suspected that some sort of contamination was the cause. Most of the damage occurred after the discharge tube was opened for one reason or another to atmospheric air (i.e. replacing damaged windows, repairing leaky bulkhead connections, etc.). Several steps were taken to try to limit the damage. First, when the gas system was re-evacuated, it was done very slowly - that way if any contaminants had entered the tube while it was open to air, they would exit the tube without striking the window. The waveguide tube was also cleaned with alcohol and a pipe cleaner, it was found that a great deal of dust had contaminated the tube. Lastly, if the tube had to be re-opened to air, the air was let in very slowly in order to limit the "rushing in" of any contaminants. These steps did limit the damage; however, the spots were always present, and causing losses in the output of the laser.

A second area that caused some problems was the slow fall time of the detector. Notice that in Figure 20

-72-

(dashed curve), the power does not even fall to zero, although that no lasing occurred at all in region II. If this response time is not taken into account, one could very easily misinterpret the data. Therefore, to find where the lasing stopped, one must find the usually sharp, "knee-of-the-curve." An extremely fast detector is necessary in order to accurately detect the lineshape of a tuned line. A HgCdTe detector proved adequate, whereas, a TGS pyroelectric did not.

Laser reflections off of the Brewster windows were a cause for concern during a portion of the thesis experiment. Because the Brewster windows were changed a number of times, it was easy to get the window mounts out of alignment. One day it was noticed that there were burn marks on the inside of the lid of the plexiglass safety shield. Reflections off the Brewster window coupled out as much as 0.8 W of laser power. Therefore, since substantial powers can be reflected off of the Brewster windows, always operate the laser with the lid on just in case stray output coupling does occur. Extensive care should also be taken to assure that the Brewster windows are aligned properly.

Finally, one minor problem that was encountered was the transfer of noise (vibrations) from the mirror clamp stands to the laser output. If the clamp stands were

tapped or leaned upon, noise (jitter) appeared in the laser output. The clamp stands were necessary to move the mirror mounts about easily. However, once the laser becomes a diagnostic tool rather than an experiment (i.e. the mirrors will be set at a fixed distance), the mirror mounts can be bolted directly to the U-beam which holds the laser. It must be noted that while the clamp stands could transfer vibrations, their performance in providing both mobility and mechanical stability of the mirror mounts was very adequate, especially when care was taken not to disturb the stands.

V CONCLUSIONS AND RECOMMENDATIONS

Conclusions

The CO_2 waveguide laser has proven itself to be a reasonably stable medium pressure laser capable of both inter-line and intra-line tuning. Its stability in intra-line tuning is especially praiseworthy when the laser's simplistic construction using inexpensive materials is considered. The range of gas pressures in the gas discharge extended from 25 Torr to 162 Torr; the latter pressure exceeded the performance of a similar laser (Ref 14) by 50 percent.

The laser, using a 20/10/70 gas mixture of $CO_2/N_2/He$, was operated in three configurations: multi-line lasing, inter-line tuning, and intra-line tuning. The multi-line configuration, which consisted of two spherical reflectors and the waveguide, produced 7.5 W of laser output. It was found that the maximum output was achieved when the mirrors (each R = 25 cm), were placed 27.5 cm from the ends of the waveguide. R = 25 cm mirrors were not the optimum mirrors to use, but they were the best available. Design theory states that for a waveguide having an i.d. = 2.4 mm, each mirror should have a radius of curvature equal to 35 cm. Therefore, if an optimum system is to be built, R = 35 cm mirrors should be used.

The resonator for the inter-line tuning configuration consisted of one spherical reflector, an AR coated germanium lens, a reflection grating, and the waveguide tube. The gas pressure and discharge current that were optimum for the multi-line configuration, were also optimum for inter-line tuning. Individual lasing lines included the P(6) to P(42) and R(6) to R(38) lines of the 10-4 μm band as well as the P(14) to P(30) and R(16) to R(24) lines of the 9.4 μm band. This wide variety of available lasing lines makes the laser an excellent tunable source. The output power extended from a few hundred milliwatts on the outlying lines up to 2.2 W on the central P(20) line. The only lens that was available in the laboratory had a focal length, f = 6.4 cm. While the lens was adequate in performance (it was used to collimate the laser beam onto the grating), a lens with a focal length of 35 cm would have been optimum.

A piezoelectric transducer (PZT) was used to hold the output coupler when the laser was set up for intra-line tuning; other than the introduction of the PZT, the resonator remained the same as it was for inter-line tuning. When a ramp voltage was applied to the PZT, the output mirror translated along the longitudinal axis of the laser about 9 μm, which permitted the scanning of nearly two free spectral ranges (FSR).

Intra-line tuning with the CO_2 waveguide laser was extremely successful. The P(20) line had a tunable linewidth of 215 MHz, which was limited by the FSR of 224 MHz. The linewidth could be varied simply by changing the discharge pressure of the laser. By controlling the pressure, one could in essence "dial-a-linewidth." The lineshape of the scanned line was very consistent from one sweep to the next, and very reproducible. Although the lineshape was somewhat asymmetric, the asymmetry does not cause any substantial degradation to the intra-line tuning.

The mechanical stability of the laser was outstanding during intra-line tuning. When the sweep time of the PZT took 50 seconds, only a very small amount of jitter was detected in the laser output. Since the system was built with inexpensive materials and no attention was given to insulating the laser from possible sources of vibration, the lack of significant jitter in the output makes the CO_2 waveguide laser a very nice diagnostic tool.

The gas absorption experiment that was conducted, was very useful in two ways. First, as the laser beam was passed through the gas absorption cell, the absorption of the beam varied as a function of the voltage applied to the PZT. This indicated, beyond a doubt, that intra-line tuning of the laser beam was occurring. Secondly, since the Voigt width (FWHM) of the absorption curve could be

measured from the data, as well as be calculated from theory, it was possible to verify that the PZT was scanning across the FSR, and that the frequency range between power minima was, in fact, a representation of the FSR.

A second lasing medium containing a 9.9/9.8/80.3 gas mixture of $N_2O/N_2/He$ was also used in the multi-line configuration. A maximum output power of 825 mW was achieved. This low output power was attributed to a poor ratio of the gases in the gas mix, as well as the less than optimum mirrors that were available. When the laser beam was analyzed with a monochrometer, the P(21) line of N_2O appeared to be the dominant lasing line. A number of other lines, P(13) to P(29) were observed to lase when the resonator was intentionally perturbed. Attempts were made to lase in the single-line configuration, however, no lasing was observed.

Overall, it is obvious that the CO_2 waveguide laser performed better than the N_2O version. In the multi-line configuration, the output power was much higher. The CO_2 laser was also capable of both inter-line and intra-line tuning, whereas the N_2O laser was not. However, since the N_2O lasing band is a little farther out in the IR (the P(21) line of N_2O is near the P(44) line of CO_2), it does provide a resonable amount of power at

-78-

wavelengths where the present CO_2 laser can not. If N_2O could be made to lase in the inter-line configuration, it would compliment the CO_2 laser extremely well.

Recommendations

The performance of the CO_2 waveguide laser was superb; however, each of the three configurations can be made to perform even better. In the multi-line configuration, each mirror should have a radius of curvature, R, equal to 35 cm, instead of the present 25 cm mirrors. Using R = 35 cm mirrors will reduce the coupling losses from about 11 to 1.5 percent. The reflectivity of the output mirror should either be 85 or 90 percent to achieve maximum output. Likewise, the new mirrors should be placed approximately 35 cm from the ends of the waveguide. Recall that the maximum laser output occurs when the mirrors are placed a distance equal to its radius of curvature away from the guide. Finally, new Brewster windows should be put on the waveguide, so that the burn spots do not affect the performance of the laser.

The inter-line tuning cavity can also be improved. The output mirror should have a R = 35 cm to minimize coupling losses, and it should be placed approximately 35 cm from the end of the waveguide in order to optimize the output power. The present short focal length lens should

-79-

be replaced with a lens of a focal length equal to 35 cm.
Replacing the old lens and positioning the new lens and
the grating approximately 35 cm from the guide will
provide maximum performance. A 95 percent reflector
should allow the maximum inter-line tunability.

To greatly improve the intra-line tuning character-
istics of the CO_2 waveguide laser, some substantial
changes must be made. Presently the P(20) linewidth is
limited by the 224 MHz free spectral range. Certain
experiments in the laboratory require a tunable linewidth
of approximately 500 MHz, therefore the length of the
laser must be reduced. With the present waveguide
(i.d. = 2.4 mm), this is not possible. However, another
waveguide (i.d. = 1.6 mm) could be used to satisfy the
tunability requirements.

Waveguide laser design theory (Degnan's case III)
tells us that for a guide of radius, a = 0.8 mm, the
output mirror should have a radius of curvature, R = 15.7
cm. Since a local power maximum exists when the mirror is
placed a distance z = R/2 from the end of the waveguide,
this distance would be approximately 8 cm. An optimum
lens – keeping tunability, not output power in mind –
would have a focal length of approximately 8 cm and would
be placed one focal length from the guide. The present
lens (f = 6.4 cm), although not optimum, would probably be

adequate to use in this configuration. If the waveguide were made to be 12 cm long, the total resonator would be approximately 28 cm in length. This would allow for a maximum tunable linewidth of 536 MHz.

If the N_2O waveguide laser could be improved so that it could operate in the inter-line tuning configuration, it would be a great compliment to the CO_2 laser. As it stands now, the 9.9/9.8/80.3 gas mixture of $N_2O/N_2/He$ is probably far from optimum. Therefore, it is recommended that a manifold be set up so that gas mix can be varied until the optimum mixture is found. The multi-line configuration with R = 35 cm mirrors should be used for this purpose. Once the best mixture has been obtained, another attempt at inter-line tuning should be made.

Finally, there were subjects that could not be investigated because of the limited time available. These areas deserve study and should be investigated in the future. No study was made of the laser beam's characteristics. What was its divergence? What was the beam's profile like? And what sort of transverse mode structure is there in the operating laser. Lastly, what causes the asymmetry in the lineshape of the output during intra-line tuning? These questions need to be answered in order to fully appreciate an operating waveguide laser.

Bibliography

1. Siegman, A.E. An Introduction to Lasers and Masers. New York, NY McGraw-Hill Book Company, 293-345 (1971).

2. Degnan, J.J. "The Waveuide Laser: A Review," Applied Physics, 11:1-33 (Nov. 76).

3. Marcatili, E.A.J. and R.A. Schmeltzer. Bell Systems Technical Journal, 43:3783 (1964).

4. Degnan, J.J. Applied Optics, 12:1026 (1973).

5. Abrams, R.L. IEEE Journal of Quantum Electronics, QE-8:838 (1972).

6. Degnan, J.J. and D.R. Hall. IEEE Journal of Quantum Electronics, QE-9:90 (1973).

7. Kogelnik, H. and T.Li. Applied Optics, 5:1550 (1966).

8. Chester, A.N. and R.L. Abrams. Applied Physics Letters, 21:576 (1972).

9. Svelto, O. Principles of Lasers, Second Edition. New York, NY Plenum Press (1982).

10. Cheo, P.K. "CO_2 Lasers," Lasers. New York, NY Marcel Dekker, Inc. 111-261 (1971).

11. Handbook of Lasers. Cleveland, OH The Chemical Rubber Co. 342-344 (1971).

12. Abrams, R.L. Applied Physics Letters, 25:304 (1974).

13. Van Lerberghe, A. et al. IEEE Journal of Quantum Electronics, QE-14,7:481-486 (1978).

14. Gerlach, R. and N. Amer. "Novel CO_2 N_2O Waveguide Laser," Scientific Instruments, 50(12):1539-1541 (Dec. 1979)

15. Hecht, E. and A. Zajac. Optics. New York, NY Addison-Wesley Publishing Company, Inc. 245 (1979).

16. Klein, M.V. Optics. New York, NY John Wiley & Sons, Inc. 493-494 (1970).

17. Hengehold, R. "Classnotes, PH 6.42 Optical Diagnostics Laboratory," unpublished, 66-74 (1982).

18. Yariv, A. _Introduction to Optical Electronics: Second Edition_. New York, NY Holt, Rinehart and Winston (1976).

19. Roth, A. _Vacuum Technology_. Amsterdam, Netherlands. North-Holland Publishing Company (1978).

20. Mantz, A.W. _Journal of Molecular Spectroscopy_, 74:339 (1979).

21. Ludwig, C.B. et al. _Handbook of Infrared Radiation from Combustion Gases_. NASA SP-3080 (1973).

22. Abramowitz, M. and I.A. Stegun. _Handbook of Mathematical Functions_. National Bureau of Standards 299 (1972).

23. Whiting, E.E. _Journal of Quantitative Spectroscopy and Radiative Transfer_, 8:1379-1384 (1968)

VITA

Adam Robert Bigelow was born on 8 October 1960 near Media, Pennsylvania. He graduated from Penncrest High School in 1978 after spending 13 months in Denmark as a foreign exchanges student. He attended the Pennsylvania State University, from which he received the degree of Bachelor of Science in Electrical Engineering on 29 May 1982. On the same morning, he also received his commission as an officer in the United States Air Force. Lt. Bigelow entered active duty and the Air Force Institute of Technology in June 1982 where he pursued his Master of Science Degree in Electrical Engineering. In November, 1983 he became engaged to Miss Paula E. Johnson of Fairborn, Ohio and they will be married in August, 1984.

Permanent Address: 629 Mizzen Avenue
                    Beachwood, NJ 08722

REPORT DOCUMENTATION PAGE

1a. REPORT SECURITY CLASSIFICATION	1b. RESTRICTIVE MARKINGS
Unclassified	

2a. SECURITY CLASSIFICATION AUTHORITY	3. DISTRIBUTION/AVAILABILITY OF REPORT
	Approved for public release; Distribution unlimited.
2b. DECLASSIFICATION/DOWNGRADING SCHEDULE	

4. PERFORMING ORGANIZATION REPORT NUMBER(S)	5. MONITORING ORGANIZATION REPORT NUMBER(S)
AFIT/GEO/PH/83D-1	

6a. NAME OF PERFORMING ORGANIZATION	6b. OFFICE SYMBOL (If applicable)	7a. NAME OF MONITORING ORGANIZATION
School of Engineering	AFIT/EN	

6c. ADDRESS (City, State and ZIP Code)	7b. ADDRESS (City, State and ZIP Code)
Air Force Institute of Technology Wright-Patterson AFB, Ohio 45433	

8a. NAME OF FUNDING/SPONSORING ORGANIZATION	8b. OFFICE SYMBOL (If applicable)	9. PROCUREMENT INSTRUMENT IDENTIFICATION NUMBER
Energy Conversion Branch	AFWAL/POOC-3	

8c. ADDRESS (City, State and ZIP Code)	10. SOURCE OF FUNDING NOS.			
	PROGRAM ELEMENT NO.	PROJECT NO.	TASK NO.	WORK UNIT NO.
Aero Propulsion Laboratory Wright-Patterson AFB, Ohio 45433				

11. TITLE (Include Security Classification)
See Box 19

12. PERSONAL AUTHOR(S)
Adam R. Bigelow, Second Lieutenant, United States Air Force

13a. TYPE OF REPORT	13b. TIME COVERED	14. DATE OF REPORT (Yr., Mo., Day)	15. PAGE COUNT
MS Thesis	FROM _____ TO _____	1983, December	93

16. SUPPLEMENTARY NOTATION

Approved for public release: IAW AFR 190-17.

LYNN E. WOLAVER 7 Feb 84
Dean for Research and Professional Development (ATC)
Wright-Patterson AFB OH 45433

17.	COSATI CODES		18. SUBJECT TERMS (Continue on reverse if necessary and identify by block number)
FIELD	GROUP	SUB. GR.	CO_2 Laser, Tunable Laser, N_2O Laser
20	05		Waveguide Laser

19. ABSTRACT (Continue on reverse if necessary and identify by block number)

Title: STUDY OF A TUNABLE CO_2/N_2O MEDIUM PRESSURE WAVEGUIDE LASER

Thesis Chairman: William Bailey, Lt Col, USAF

20. DISTRIBUTION/AVAILABILITY OF ABSTRACT	21. ABSTRACT SECURITY CLASSIFICATION
UNCLASSIFIED/UNLIMITED ☒ SAME AS RPT ☐ DTIC USERS ☐	Unclassified

22a. NAME OF RESPONSIBLE INDIVIDUAL	22b. TELEPHONE NUMBER (Include Area Code)	22c. OFFICE SYMBOL
William F. Bailey, Lt Col, USAF	(513) 255-2012	AFIT/ENP

DD FORM 1473, 83 APR   EDITION OF 1 JAN 73 IS OBSOLETE.   UNCLASSIFIED

SECURITY CLASSIFICATION OF THIS PAGE

Abstact: The operational characteristics of CO_2 waveguide laser, capable of both inter-line tuning and intra-line tuning, were investigated. This system based on the work of Gerlach and Amer exhibits an overall simplicity in design and construction. In addition, only inexpensive and readily available materials are required. The range of gas pressures in the discharge tube extended from 25 Torr to 162 Torr while using a 20/10/70 gas mixture of $CO_2/N_2/He$. The P(20) line, which was scanned using a piezoelectric transducer, had a tunable linewidth of 215 MHz. This linewidth was limited by the 220 MHz free spectral range of the cavity. In the multi-line configuration, the maximum output was 7.5 W. A grating was used to achieve inter-line tuning; a total of 50 different lines of the P and R branches of the 10.4 m and 9.4 m bands lased. A maximum output power of 2.2 W, P(20), was achieved during single line operation. A 9.9/9.8/80.3 gas mixture of $N_2O/N_2/He$ was also investigated. In the multi-line configuration, a maximum output of 825 mW was achieved.

FILME
4-84